

## **UWL REPOSITORY**

**repository.uwl.ac.uk**

Coupling Behaviour of Autogenous And Autonomous Self-Healing Techniques  
for Durable Concrete

Shaaban, Ibrahim ORCID: <https://orcid.org/0000-0003-4051-341X> (2024) Coupling Behaviour of Autogenous And Autonomous Self-Healing Techniques for Durable Concrete. *International Journal of Civil Engineering*, 22. pp. 925-948. ISSN 1735-0522

<http://dx.doi.org/10.1007/s40999-023-00931-4>

This is the Accepted Version of the final output.

**UWL repository link:** <https://repository.uwl.ac.uk/id/eprint/10629/>

**Alternative formats:** If you require this document in an alternative format, please contact: [open.research@uwl.ac.uk](mailto:open.research@uwl.ac.uk)

**Copyright:** Creative Commons: Attribution 4.0

Copyright and moral rights for the publications made accessible in the public portal are retained by the authors and/or other copyright owners and it is a condition of accessing publications that users recognise and abide by the legal requirements associated with these rights.

**Take down policy:** If you believe that this document breaches copyright, please contact us at [open.research@uwl.ac.uk](mailto:open.research@uwl.ac.uk) providing details, and we will remove access to the work immediately and investigate your claim.

# Coupling Behaviour of Autogenous And Autonomous Self-Healing Techniques for Durable Concrete

Ahmed Hassanin<sup>1,2</sup>, Amr El-Nemr<sup>3</sup>, Hesham F. Shaaban<sup>4</sup>, Messaoud Saidani<sup>5</sup> and Ibrahim Shaaban<sup>6,\*</sup>

[aihnnng@missouri.edu](mailto:aihnnng@missouri.edu)<sup>1</sup>, [ahmed-ibrahim@eru.edu.eg](mailto:ahmed-ibrahim@eru.edu.eg)<sup>2</sup>, [amr.elnemr@guc.edu.eg](mailto:amr.elnemr@guc.edu.eg)<sup>3</sup>,  
[hmshaban@eng.zu.edu.eg](mailto:hmshaban@eng.zu.edu.eg)<sup>4</sup>, [cbx086@coventry.ac.uk](mailto:cbx086@coventry.ac.uk)<sup>5</sup>, [ibrahim.shaaban@uwl.ac.uk](mailto:ibrahim.shaaban@uwl.ac.uk)<sup>6</sup>

## Abstract

Recent research on self-healing concrete has shown some drawbacks and conflicts between the different techniques such as difficulty in casting, healing agent release, preparation complexity, high safety requirements against bacteria protection, undesirable expansion, and uncertainty in healing product generation. Despite these limitations, the hybrid technique was suggested and showed promising results. This paper explores the hybridization of the two techniques; autonomous and autogenous by utilizing the *B. subtilis* bacteria, mineral admixtures like fly ash, and Polyvinyl alcohol fibers (PVA) together. The experimental program involves assessing the self-healing efficiency when coupling the bacteria, fly ash, and PVA fiber by assigning six mixtures, including a control OPC. The six mixtures encountered the Bacteria addition at certain concentrations and varying PVA fiber percentages; 1, 1.5, and 2% while partially replacing the cement replacement with 20% fly ash, while the last mixture combines both the bacteria, fly ash and 1% PVA fiber. Mechanical properties such as compressive and flexural strength, in addition to, water absorption and sorptivity as transport properties were examined for concrete repair and restoration purposes. The results reveal that the *B. subtilis* bacteria significantly enhance the compressive and flexural strength recovery along with lowering sorptivity and absorption rate compared to those with PVA addition when exposed to wet and dry cycles of curing at 28 days of age. The coupling effect, on the other hand, provides a substantial gain in strength of 63% at a longer age (56 days), indicating the potential of this approach for long-term concrete repair. Despite the challenges of the *B. subtilis* survival bacteria, the coupling of both bacteria and PVA fiber demonstrates superior performance in maintaining the durability of repaired concrete in the long term.

Keywords: self-healing techniques; absorption; durability; mechanical properties; concrete repair; crack widths.

## Compliance with Ethical Standards

- The authors declare that they have no conflict of interest.
- This article does not contain any studies with human participants or animals performed by any of the authors.
- The authors declare that they have no known competing financial interests or personal relationships that could have appeared to influence the work reported in this paper.
- The authors state that they did not get any funding for this research and it is self-funded.

<sup>1</sup> Postdoctoral Fellow, Civil and Environmental Engineering Dept., University of Missouri-Columbia, USA.

<sup>2</sup> Lecturer, Engineering Construction Dept., Faculty of Engineering, Egyptian Russian University-Cairo, Egypt.

<sup>3,\*</sup> Associate Professor in Material Engineering, Civil Engineering Program, German University in Cairo (GUC), Cairo, Egypt.

<sup>5</sup> Professor of Structural Engineering and Dean, National Zagazig University, Egypt.

<sup>5</sup> Associate Director of Research and Engagement, Coventry University, UK.

<sup>6,\*</sup> Programme Director, University of West London, UK.

# Coupling Behaviour of Autogenous And Autonomous Self-Healing Techniques For Durable Concrete

## Abstract

Recent research on self-healing concrete has shown some drawbacks and conflicts between the different techniques such as difficulty in casting, healing agent release, preparation complexity, high safety requirements against bacteria protection, undesirable expansion, and uncertainty in healing product generation. Despite these limitations, the hybrid technique was suggested and showed promising results. This paper explores the hybridization of the two techniques; autonomous and autogenous by utilizing the *B. subtilis* bacteria, mineral admixtures like fly ash, and Polyvinyl alcohol fibers (PVA) together. The experimental program involves assessing the self-healing efficiency when coupling the bacteria, fly ash, and PVA fiber by assigning six mixtures, including a control OPC. The six mixtures encountered the Bacteria addition at certain concentrations and varying PVA fiber percentages; 1, 1.5, and 2% while partially replacing the cement replacement with 20% fly ash, while the last mixture combines both the bacteria, fly ash and 1% PVA fiber. Mechanical properties such as compressive and flexural strength, in addition to, water absorption and sorptivity as transport properties were examined for concrete repair and restoration purposes. The results reveal that the *B. subtilis* bacteria significantly enhance the compressive and flexural strength recovery along with lowering sorptivity and absorption rate compared to those with PVA addition when exposed to wet and dry cycles of curing at 28 days of age. The coupling effect, on the other hand, provides a substantial gain in strength of 63% at a longer age (56 days), indicating the potential of this approach for long-term concrete repair. Despite the challenges of the *B. subtilis* survival bacteria, the coupling of both bacteria and PVA fiber demonstrates superior performance in maintaining the durability of repaired concrete in the long term.

Keywords: self-healing techniques; absorption; durability; mechanical properties; concrete repair; crack widths.

## 1. Introduction

Concrete exhibits cracking as the sustained service load is applied which develops tensile stresses at the extreme fiber of the beam element or excessive compression load on compression element as columns. These cracks might inevitably find their path through the porousness of the concrete. Hence, this cracking would shorten the durability and damage the endurance life of the structures, in addition to the maintenance cost that would be required to repair or rehabilitate the damaged structure [1]. Eventually, this cracking has different causes and possesses various paths, however, they commonly start internally through microcracking and end up with concrete fracture, in addition to steel reinforcing bars experiencing corrosion, especially structures in coastal areas [2]. Generally, infrastructures that are more than 50 years old are susceptible to deterioration and comprehensively require maintenance [3]. Japan adopted self-healing as a promising technique when dealing with inherent cracks in concrete elements [4, 5].

The self-healing techniques are divided into two main techniques; autogenic and autonomic self-healing of the concrete. Several investigations reported that small cracks in concrete can heal under the effect of 'autogenous healing' or 'self-healing' of concrete. Usually, this action takes place through, physical, and mechanical processes of the concrete mix ingredients based on calcite crystallization to form calcium carbonate along with water and CO<sub>2</sub> [4 - 6] without using any external stimulation, however, crack closure can reach less than 0.18 mm. On the contrary, the cracks repaired autonomously usually incorporate a specific healing agent within the matrix which varies in type and chemical-based mechanism. Recently the possible addition of bacteria admixture, micro additives, micro-grains, microcapsules, and nanomaterials without external intervention as the self-healing agent has also been considered. Wiktor & Jonkers [7] and Nishiwaki et al. [8] reported that incorporating the bacteria involves calcium carbonate as a biological precipitation of cracks through the CO<sub>2</sub> reaction. Their research aimed to quantify the healing potential of two-bio-chemical self-healing agent components embedded in expanded clay particles, acting as reservoir particles and partially replacing coarse aggregate. These components are released by crack ingress water and fill the cracks in the concrete mixture.

On the other hand, many researchers [9 - 15] investigated other methods for triggering the healing agents (adhesives) whether embedded in capsule or vascular networks as the mixing process. Nishiwaki et al. [8, 9] used a heating device that triggered parts of concrete through pipes with a plastic organic film encapsulated by the repair agent which releases as soon as it melts when heating filling the crack and hardening, recovering the strength of the concrete mixture. Their concerns lie in the bacteria's survival within the concrete matrix as the concrete process from the mixing and pouring environment might not be appropriate for their survival with additional concerns about long-term survival through the life cycle of the structure [8, 9]. Another study by Dry [10] reported the timing and location release of sealants, adhesives, and waterproofing encapsulators placed internally to acquire the durability required. Their results showed that some of these encapsulations may appear in the fibers but could possess the chemicals where and when the matrix cracks, causing the fiber to crack and release chemicals. Tittelboom et al. [11] explore the utilization of computed tomography and visual observation of crack faces while using an encapsulated healing agent embedded in the mortar matrix to obtain self-healing properties. Their results showed the cracks filling with a healing agent and more than 50% of strength was recovered. Further, they reported that the water permeability would reduce and hence the proposed autonomic technique can resort partially to the concrete properties.

Joseph et al. [12] investigated the addition of adhesive-filled glass reservoirs as self-healing agents on reinforced mortar beams subjected to two cycles of loading. The results revealed that there was evidence of crack-healing following the first loading cycle and new crack formation during the second loading cycle, in addition, to secondary healing for the new secondary cracks. They were motivated to provide more data for the long term in terms of numerical methods. Homma et al. [13] explain the utilization of three fibers (polyethylene (PE), steel cord, and hybrid composites) to examine the self-healing properties of fiber reinforced cementitious composites (FRCC) through cracking using tension test and retained at 28 days after water curing. Their results revealed that the PE fiber has provided the most influence based on the volume in bridging the crack and crystallization products attached easily to the larger numbers of PE fibers, in addition to the reduction in permeability coefficient that was achieved. They observed the hydration degree has a slight influence on the self-healing capability.

Nishiwaki et al. [14] have examined other various types of synthetic fibers that have different chemical properties such as polyvinyl alcohol (PVA), ethylene vinyl alcohol (EVOH), polyacetal (POM), and polypropylene (PP) on FRCC evaluating the self-healing capability of FRCC. Their microscopic results showed the fibers' polarity provided a bridging crack through self-healing precipitation and filled the cracks, in addition, reduced the water permeability coefficient and in some cases no water tightness recovery. Nevertheless, they ensured that the chemical properties of the fibers and geometrical properties of the crack surface from roughness, complexity, and continuity of the fibers influence the self-healing properties in terms of water tightness. Mauser et al. [15] stated that the autogenous methods mainly depend on mineral admixtures such as fly ash and fiber addition, such as polyvinyl alcohol (PVA) fibers. Their investigation revealed that these additives have great potential for the self-healing process in concrete and provide good results in real applications under certain curing conditions. These fibers could help in enhancing self-healing through the process of controlling the crack and accelerating  $\text{CaCO}_3$  precipitation. Recent studies by Liang et al. [16] and Hammad et al. [17] showed that these fibers (PVA) have provided high polarity synthetic composite and act as a bridge through the crack [17].

Although the above-mentioned techniques are widely used, several researchers [18 – 21] observed various challenges and limitations when applying mineral admixture and PVA additives, utilizing the triggers and microcapsules systems. These challenges can be limited by the chemical triggers existing within the solution and along the fibers including, pH values and ions charge on the fiber surfaces. For instance, Dong et al. [18] established a microcapsule system to contain the chemical self-healing for cementitious composites. The survival challenges could be overcome by capsulation; however, it is required to hatch the healing agent through activation of the healing process. Method of the EDTA (Ethylene Diamine Tetra- acetic Acid) titration method was utilized to release the corrosion inhibitor healing agent from the microcapsule covered by polystyrene resin (PS). This is functioned by time and wall thickness of the microcapsule. Nevertheless, the corrosion inhibitor release rate is noticeably influenced by the pH value which increases with the decreasing pH value, which is a bit not controllable. On the other hand, Lv et al. [19] developed a polymeric microcapsule type utilizing the phenol formaldehyde (PF) resin as a shell and dicyclopentadiene (DCPD) as a healing agent for self-healing microcracks in cementitious materials. Their results provided that the microcapsules have excellent stability in hatching the microcapsules by crack trigger and releasing the healing agent in a stable manner healing the cracks simultaneously, however, no rate or insurance that the microcapsules will survive for the long term was explored or investigated. Xu et al. [20] used ultrasonic wave-induced to trigger the microcapsules for healing agent release. They found that this method was controllable and cost-effective. The results revealed the strength recovery for mixes triggered by ultrasonic were 2 – 4 times higher than mechanical-triggered ones. Yet still it is not manageable to trigger the healing agent by ultrasonic.

Consequently, although several trials were proposed to overcome the survival problems using trigger additives, vessels, and microcapsules, other researchers [21, 22] have suggested having the coupled effect using fibers and bacterial admixtures. Feng et al. [21] investigated the utilization of hybrid techniques by using bacteria and fiber as it has the potential to enable excellent self-healing performance in concrete. Their experimental program studied the coupled effect of PP fiber, PVA fiber, and bacteria on the self-healing efficiency of concrete. The results revealed that PP and PVA fiber would reduce the bacteria

concentration. The crack width of 300–500  $\mu\text{m}$  was healed within specimens with bacteria and fiber than that with bacteria only. Further, the water tightness and flexural strength recovery were improved as a result of calcium leaching and calcium ions utilization deposition on fiber surfaces. In addition, they found that the PVA fibers filled the cracks with polarity groups and cell structure of polyvinyl alcohol fiber on calcium carbonate nucleation. Furthermore, Qiu et al. [22] studied the inclusion of slag-based ECC as it has the potential for autogenous healing. Several factors: slag content, crack width, and environmental alkalinity, on the efficiency of the autogenous healing of ECC were explored. They observed that the single-cracked ECC specimens with different slag content and crack width under conditioned underwater or NaOH/dry cycles. The healing results revealed the coupling effects of crack width, slag content, and alkalinity conditions. However, drawbacks such as limited maximum allowable crack width which could be only partial or no healing. The  $\text{CaCO}_3$  could be produced as the main healing component under water/dry conditioning while the NaOH/dry cycles condition initiates the slag hydration for 24 hours and results in the formation of C-S-H and  $\text{CaCO}_3$ . It is concluded that  $\text{CaCO}_3$  precipitation is more effective in engaging autogenous healing than the formation of C-S-H. The concept of associating allowable crack width and slag content is proposed, which would guide ingredient selection and component tailoring to engage robust autogenous healing in ECC in the future.

In the previous studies, the coupling effect of the two techniques autogenous and autonomous has the potential to overcome many challenges instead of utilizing other chemical additives or encapsulated systems. Yet still fewer researchers explored this combination as mentioned earlier. Nevertheless, gaps remain not demonstrated on the impact of the autonomous in comparison to autogenous self-healing in repairing the pre and post-cracking of the damaged elements and the restoration of their mechanical properties. Thus, this study explores the coupling effect utilizing bacteria, PVA fibers, and mineral admixtures such as fly ash, observing the improved properties and self-healing capacity of concrete in terms of mechanical properties restoration represented in compression and flexural strength. In addition, it introduces the hybridization techniques of the two self-healing techniques to stand on their impact in enhancing and restoring the compression and flexural strength of the cube and prism specimen as a demonstration for further investigation of structural elements under operation while managing to explore the durability performance of the self-healed produced concrete using permeability and water absorption tests.

## 2. Research Significance

Recent literature compares the results of the two available techniques: autonomic and autogenous with other systems to trigger the healing agent whether through encapsulation or vessel system. Usually, the aim is to overcome the many challenges from bacteria survival or healing agent release on time and location of repairing the crack. Other drawbacks involve the bacteria accommodation in the concrete mixture. The deposition of  $\text{CaCO}_3$  on the surface of the fiber made the possibility of achieving the location and timing required by the bacteria with the contribution of mineral admixtures such as fly ash and PVA fibers to bridge the crack and fill it. This potential motivates the study to explore more about the pre and post-cracking of the concrete specimens within the mechanical properties in terms of compressive and flexural strength at long aging. This action would ensure crack closure and an impermeable concrete surface for absorbing hazards and deleterious

materials affecting the reinforcement with corrosion and other defects especially in the coastal environment.

### 3. Experimental Program

#### 3.1 Materials and Mix Design

##### 3.1.1 Cement

The cement used was Ordinary Portland Cement, grade 42.5 MPa (N/mm<sup>2</sup>). The cement's properties are compatible with European standards EN 197 [23] and Egyptian standards (4756-1 /2007) [24] as provided by the manufacturer. The physical, chemical, and mechanical properties of the cement are described in Table 1.

##### 3.1.2 Fly Ash

Fly ash class F originates from anthracite and bituminous coals. It consists mainly of alumina and silica. Class F fly ash has a lower calcium content than Class C fly ash. The rest of its chemical composition is presented in Table 1. The Additional chemical requirements as per ASTM C 618 [25] are listed in Table 1.

##### 3.1.3 Fine and Coarse Aggregate

Natural siliceous sand was used as fine aggregate, and crushed dolomite stone was used as coarse aggregate. Fig. 1 shows the grain size distribution of combined fine and coarse aggregates. As deduced from Fig. 1, the nominal aggregate size was 12.5 mm. The physical and chemical properties of fine and coarse aggregates are also represented in Table 2.

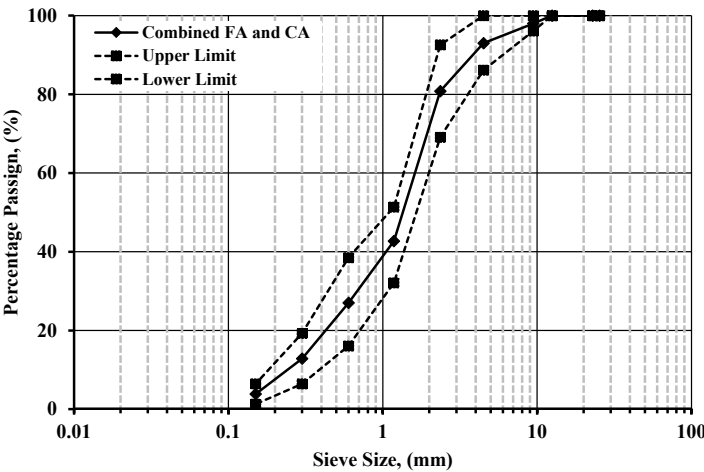


Fig. 1. Sieve analysis of fine and coarse combined aggregate with limit ASTM C33[26]

The fine aggregate utilized silica sands for applications other than building because of their high silica content (more than 95% SiO<sub>2</sub>). Silica sands include a significant quantity of quartz, abundant in silica, and, more importantly, relatively little clay, iron oxides, or chromite, a refractory mineral. Their grain size distribution is typically restricted (0.1 to 2 mm).



**Table 1.** Physical, chemical, and mechanical properties

| <b>Chemical composition in (%)</b>   |            |                       |   |
|--------------------------------------|------------|-----------------------|---|
| <b>Component (%)</b>                 | <b>OPC</b> | <b>FA<br/>Class f</b> | <b>ASTM C 618 [25]<br/>Requirements (%)</b> |
| SiO <sub>2</sub>                     | 47.09      | 47.09                 | 70  |
| Al <sub>2</sub> O <sub>3</sub>       | 17.41      | 17.41                 | 70  |
| Fe <sub>2</sub> O <sub>3</sub>       | 8.34       | 8.34                  | 70  |
| CaO                                  | 13.98      | 13.98                 | -   |
| MgO                                  | 1.85       | 1.85                  | -   |
| SO <sub>3</sub>                      | 4.65       | 4.65                  | -   |
| Na <sub>2</sub> O                    | 2.44       | 2.44                  | -   |
| K <sub>2</sub> O                     | 1.8        | 1.8                   | -   |
| Loss ignition                        | 2.2        | 1.79                  | -   |
| <b>Physical properties</b>           |            |                       |   |
| Density (kg/m <sup>3</sup> )         | 3160       | 2150                  | -   |
| Activity index % (after 28 days)     | -          | 77.5                  | -   |
| Activity index % (after 90 days)     | -          | 85.6                  | -   |
| Specific gravity                     | 3.16       | -                     | -   |
| Initial setting time (min)           | 180        | -                     | -   |
| Soundness (mm)                       | 1          | 1                     | -   |
| Fineness %                           | -          | 22.43                 | -   |
| Water Absorption (%)                 | 32         | -                     | -   |
| loss of ignition (%)                 | 2.2        | -                     | 6   |
| Sulfate content (SO <sub>3</sub> ) % | 2.7        | -                     | 5   |
| Blaine fineness (cm <sup>2</sup> /g) | 4100       | 2469                  | -   |
| Reactive SiO <sub>2</sub> %          | -          | 40.34                 | -   |
| Blaine (cm <sup>2</sup> /g)          | -          | 3330                  | -   |
| Alkalis%                             | -          | 2.46                  | -   |
| Free CaO                             | -          | 0.03                  | -   |
| Color                                | Grey       | Grey<br>(blackish)    | -   |
| <b>Compressive strength (MPa)</b>    |            |                       |   |
| <b>Mechanical properties</b>         |            |                       |   |
| 1 day                                | 25         | -                     | -   |
| 2 days                               | 38         | -                     | -   |
| 28 days                              | 68         | -                     | -   |

Table 2 shows the physical properties of the fine and coarse aggregate used in this investigation. Sieve analysis of the combined fine and coarse aggregate used in the mix design, as shown in Fig. 1. These properties were determined according to ASTM C 33[26], BS EN 933-1 [27], ASTM C117 [28], ASTM C127[29], ASTM C128 [30], BS 812-2[31], BS 812-103 [32].

**Table 2.** Physical and chemical properties of fine and coarse Aggregate



| Physical and chemical properties |          |          |
|----------------------------------|----------|----------|
| Property                         | FA       | CA       |
| Specific gravity                 | 2.62     | 2.65     |
| Volume weight                    | 1.84 MPa | 1.73 MPa |
| Void ratio                       | 31.0%    | 33.8%    |
| Absorption percentile            | 1.6%     | 1%       |
| Fineness modulus                 | 6.62     | 2.72     |
| Clay, silt, and dust ratio       | 0.09%    | 2.0%     |
| Percent of chloride              | 0.03%    | 0.03%    |

### 3.1.4 Polyvinyl Alcohol Fiber

Polyvinyl alcohol (PVA) fiber has been used in the concrete mix as it has a very high elastic modulus and tensile strength. The properties of the fiber are listed, as shown in Table 3.

**Table 3.** Physical and technical properties of PVA fiber

| Content             | PVA      |
|---------------------|----------|
| Length              | 9 mm     |
| Diameter            | 0.04 mm  |
| Specific gravity    | 1.12     |
| Elastic modulus     | 40 GPa   |
| Tensile strength    | 1320 MPa |
| Modulus strength    | 34 (GPa) |
| Elongation at break | 6.80 %   |

### 3.1.5 Producing Bacteria and Bacterial Environment

*B. subtilis* was selected based on ease of availability and quickly cultivated. The typed culture of *B. subtilis* (ATCC23857) is a soil-found strict aerobic gram-positive, rod-shaped bacteria that can withstand high temperatures and produce spores dormant for many years. Using the MacFarland standard, the fresh bacterium strain was standardized [33] to obtain 108 cells/ml, which was used in this study as adopted by Tian et al.[33].

The bacteria were cultured and grown for the investigation using two culture mediums,  $\text{NH}_4\text{-YE}$  Nutrient Broth Medium and  $\text{NH}_4\text{-YE}$  Agar Plate Medium, besides the Tris buffer solution and other components like peptone, yeast extract, and ammonium sulfate, which create the medium of  $(\text{NH}_4\text{SO}_4)$ . The tris buffer solution was created by 16.20 grams (g) of tris (hydroxyl methyl amino meth) dissolved in about 0.5 liters (L) of distilled water to create a colorless solution that was used to create 1 liter (L) of tris buffer solution. A pH of 9.0 was achieved by titrating the solution with 1 molar hydrochloric acid (HCl). The remaining volume of 1 L was then filled with distilled water. The  $\text{NH}_4\text{-YE}$  Nutrient Broth Medium was created with 20 grams of yeast extract and 10 grams of  $\text{NH}_4\text{SO}_4$  added to one liter of tris buffer solution in a conical flask. The mixture was then thoroughly agitated until the yeast extract was dissolved. Before inoculating the test organism, the solution was autoclaved according to the usual protocol at 121 °C for 15 min. It was then allowed to cool to room temperature (25 °C). Some species generate the enzyme urease, which degrades

urea to create ammonia [2, 14, 34, 35]. The motility and indole confirmed the identity of the isolate, and urease (MIU) biochemical assays were used to validate the identification of the bacteria, as reported by Feng et al. [21].

Finally, a microscopic confirmation of the production of calcium carbonate residue was confirmed after verifying the organism's motility, indole, and urease identities using the MIU (Motility Indole Urea) test. Then, Microscopic analysis revealed the organism's capacity to precipitate calcium carbonate.  $\text{CaCl}_2\text{H}_2\text{O}$  and urea (3 g in 100 ml of sterile distilled water) were added to the nutritional solution after sterilizing it for 15 minutes at  $121^\circ\text{C}$  [2, 21]. After allowing it to cool, the organism was injected into it. Following seven days of interval incubation at the optimum temperature and pH on days 0, 7, 14, 21, and 28 on an orbital shaker, this was then studied under a microscope. The precipitation of  $\text{CaCO}_3$  by the organisms following it, which was Gram's stained and observed under the microscope, demonstrated the precipitation of calcium carbonate.

After that, a nutrient broth medium was used to subculture the *B. subtilis* strain. The medium was serially diluted to provide  $10^8$  cells/ml before being introduced using a sterile loop from the Petri plate holding the organism. The nutrient broth was injected in a ratio of 1:10 into a 250 ml conical flask that contained 200 ml of the sterile culture medium and was then covered with cotton wool and aluminum foil to prevent contamination. The culture media were incubated at  $30^\circ\text{C}$  and then moved to an orbital shaker at 130-300 revolutions per minute (rpm) for 10 days to ensure the maximum growth of the bacteria.

The test isolates and preserves the pure culture of *B. subtilis*, initially kept on nutrient agar slants, producing uneven, dry, white colonies. Before inoculating into the prepared medium, it was subculture regularly to get new culture. The culture procedure was carried out in a sterile environment [2]. Fig.2 depicts the prepared 250 ml medium (Nutrient broth) before autoclaving and the cultivated bacteria solution following shaking.



**Fig. 2. Bacterial solution**

### 3.2 Concrete mix design

The concrete mixes were designed through the ACI 211.1-91 [36], including six mixes containing bacteria, and PVA fiber added while having a control mix without any additional minerals or admixtures for comparison purposes. Three of the six mixes include PVA fibers at different volume percentiles ranging from 1 to 2%, while the sixth mix combines PVA fiber and bacteria. The other two mixes; one represents the use of OPC as control and the

other uses bacteria only. Tables 1, 2, and 3 show the physical properties of cement, fly ash, PVA fiber, and fine and coarse aggregate used for mix design. Table 4 presents the concrete mix design for a one-meter cube. The target strength of the concrete was C32 grade and the water-to-cement ratio of 0.43 for preparing the specimens. The following specimens were prepared for each test variable; 126 cubes of side dimensions of 150 mm and 108 prisms dimensioned 100 x 100 x 500 mm. The six mixtures include one control mix, one bacterial mix, three PVA mixes at different percentiles, and one combined mix, bacterial with PVA at 1.0% by volume fraction (VF). As shown in Table 4, the control mix was denoted by “OC,” while “BC” denoted the bacterial concrete mix. In addition, those with PVA were denoted by “PVAC”. While the “1” indicates the percentile of PVA fiber added. For instance, “1” means 1 percent of PVA volume fraction was added, while “1.5” and “2” stands for 1.5 and 2 percent of PVA volume fraction. Only the sixth mix was represented by “BC+PVAC1,” which combines bacterial and PVA fiber of VF of 1.0%. The selection of the volume fraction of PVA was based on the study carried out by Srinivasa et al. [37]. The study investigated the utilization of PVA from 0 to 2% through collected data from literature and found that the results are more reliable when using PVA volume fraction ranges between 1 to 2%, in addition, it provides an enhancement to compressive and tensile strength. Based on this research, it was deduced that the suitable PVA volume fraction would be between 1 to 2%, hence, three PVA volume fraction was selected, 1, 1.5, and 2%.

**Table 4.** Details of concrete mix design

| ID            | Water,<br>liter<br>/m <sup>3</sup> | Cement<br>content,<br>kg/m <sup>3</sup> | Fly<br>Ash,<br>kg/m <sup>3</sup> | Fine<br>Aggregate,<br>kg/m <sup>3</sup> | Coarse<br>Aggregate,<br>kg/m <sup>3</sup> | Bacteria  | PVA<br>Addition<br>(%) by<br>volume |
|---------------|------------------------------------|---|----------------------------------|---|---|---|-------------------------------------|
| OC            | 172                                | 400                                     | 120                              | 550                                     | 1165                                      | ---   | ---                                 |
| BC            | 172                                | 400                                     | 120                              | 550                                     | 1165                                      | Count of 1.08*10 <sup>8</sup><br>cells/ml, solution<br>concentration of 600<br>nm/liter | ---                                 |
| PVAC1         | 172                                | 400                                     | 120                              | 550                                     | 1165                                      | ---   | 1%                                  |
| PVAC1.5       | 172                                | 400                                     | 120                              | 550                                     | 1165                                      | ---   | 1.50%                               |
| PVAC2         | 172                                | 400                                     | 120                              | 550                                     | 1165                                      | ---   | 2%                                  |
| BC+<br>PVAC1* | 172                                | 400                                     | 120                              | 550                                     | 1165                                      | Count of 1.08*10 <sup>8</sup><br>cells/ml, solution<br>concentration of 600<br>nm/liter | 1.0%                                |

\*The PVA fiber Volume fraction was elected based on the optimized values in terms of workability and hardening properties of mixes with PVA fiber volume fraction mixes; PVAC1, PVAC2, and PVAC3.

### 3.3 Mixing Process

The study's objective is to observe the influence of two mechanisms, autonomic and autogenous methods, for healing the cracked concrete and developing its strength and other durability properties. In addition, the influence of replacing cement with binding materials such as fly ash on autogenous self-healing and closure of the cracks. A further combination of the two mechanisms was considered and their influences on crack closure were reported

as shown later in Fig. 3, 8, and 10. This objective was extended to observe the influence of combining the two mechanisms on the closure of concrete cracking as well.

The concrete mixtures were produced following the procedures outlined by Zhou et al.[38]. Zhou et al.[38] adopted the sequence of adding dry components from cement and fly ash first together while mixing for 2 minutes at low speed (600 rpm) in the electric concrete mixer. Then, an appropriate solids amount (2/3 of the total volume) was mixed with half of the calculated mixing water for 2 minutes at low speed. the fine aggregate (sand) was, then added incrementally over 1 minute while continuing to mix at low speed. The mixture was mixed for an additional 2 minutes after the full addition of sand. The PVA fibers were slowly added over 1 minute at low speed. The mixture was left to sit undisturbed for 1 minute without mixing. Then mix at high speed (4000 rpm) for 2 minutes to uniformly distribute the fibers. The remaining mixing water was incrementally added over 1 minute at low speed. The final mixing was conducted at high speed for 2 minutes to produce a homogenous mixture. In the case of mixtures including bacteria, the calculated bacterial solution was injected into the continuously mixing concrete using an injection device. This ensured thorough dispersion of the bacteria throughout the mixture.

### 3.4 Sample Preparation

A total of 126 cube specimens and 108 prism specimens were prepared by pouring the concrete mixes into the molds; then, the specimens were placed onto the vibrating table, ensuring the compaction of the concrete thoroughly. The specimens were left in the molds of the laboratory for 24 hours. Then, the specimens were removed from the molds and placed inside curing tanks for 7, 28, and 56 days until testing. All samples were prepared, and water cured by BS EN 12390-2 [39].

### 3.5 Details of Test Specimens

The experimental program contained four main variables representing different mixtures, including varied ratios of PVA fibers volume (1.0, 1.5%, and 2.0%), adding the bacterial solution to the mixing water with a count of  $1.08 \times 10^8$  cells/ml (solution concentration of 600 nm/liter) and ordinary concrete as a reference mix. The experimental program comprised 9 cube specimens for each mix and the cracking load was assigned accordingly to the control mix. The specimens covered the ages of 7, 28, and 56 days. Similarly, 3 scaled prisms of span 500 mm, depth 100 mm, and width 100 mm were encountered for each mix at two different ages, 28 and 56 days. 18 cubes were disturbed as follows for each durability test: sorptivity, absorption, and permeability at 7, and 28 days of age.

For assessing the gain and recovery of compressive and flexural strengths, each mix has at least 6 cube specimens at 7, 28, and 56 days of age. Three of the specimens were undamaged and the other was pre-damaged at about 60%. Then, the specimens are exposed to the healing process. The process of healing acts after cracking the specimens with an initial cracking load. The healing process adopted was wet and dry cycles of curing to assess the regain after the healing process through testing again. The duration of curing through the wet and dry cycle healing process is 28 and 56 days of age. It should be mentioned that only those specimens that were pre-damaged at 7 days of curing were exposed to a healing

process of 28 days. The others ages: 28 and 56 days were exposed to the healing process at the same curing ages; 28 and 56 days as well.

### 3.6 Test Methods

Several tests were conducted to determine the fresh and hardened state properties of the produced concrete. In addition, various durability tests were carried out to assess the durability of the concrete with PVA or bacteria. Slump tests for the fresh concrete mixes were carried out to determine the workability of the fresh concrete mixes and were conducted as per ASTM C143 / C143M [40]. Slump tests are used to measure the vertical settlement or "slump" of a standardized sample, which starts by filling with concrete the frustum cone into layers. Each layer was tamped 25 times then the mold was removed and inverted, allowing the sample to subside under its weight for 3 minutes. The slump is measured as the difference between the original height and the final settled height of the sample. The slump value indicates the concrete's consistency and flowability, with a higher slump indicating higher workability.

The density of the hardened concrete was conducted according to ASTM C642 [41] at the age of 28 days. In this test, the hardened concrete sample is weighed after an oven-dry at a temperature of 100 to 110 °C for not less than 24 hours allowing it to cool in dry air. Then the sample is weighed after being immersed in water at approximately 21 °C for not less than 48 h. Finally, the sample is placed and covered with tap water boiled for 5 h. Then the sample is allowed to cool down not less than 14 h reaching room temperature of 20 to 25 °C. The steps should be repeated at each stage until the difference between any two successive measurements is less than 0.5 % of the lowest mass obtained in the case of oven-dry and observed an increase in mass less than 0.5% of the larger mass provided in case of water saturation. The bulk density can be calculated through the equations provided by ASTM C642 [41] for oven-dry, immersed, and boiling cases

The compressive strength test measures the maximum load a concrete sample, whether cylindrical or cube, can bear before failure when loaded axially in compression. The compressive strength at a given age is evaluated by calculating the average strength of three consecutive samples. This test is carried out to determine the loading capacity of hardened concrete. However, in this study, the compressive strength was measured in two stages. The first stages included testing the control specimens till failure. Thus, the peak load can be known from the very beginning, at 7, 28, and 56 days. The second stage relies on the pre-damaged three specimens up to 60% of the peak compressive strength of the un-damaged specimens, or the corresponding load that produces a 0.1 mm crack width threshold or more [33, 42 - 44]. This pre-damaging load level ensured visible cracking was produced to initiate damage while avoiding complete crushing or pulverization of the samples. After initiating cracks at the pre-determined cracking load level, the three pre-damaged specimens were then exposed to wet and dry cycle curing methods at 7, 28, and 56 days depending on pre-damage age to allow for self-healing [33, 42 - 44]. The cracked and healed strength obtained after the curing periods was then used to evaluate the concrete mixtures' inherent healing capabilities over time at different damage levels and curing durations through compression



testing till failure or crushing of the specimen. This testing methodology provided a standardized approach to deliberately damage samples for quantification of self-healing performance. Thus, there were two stages: one un-damaged and pre-damaging three specimens for each mix at each age, as shown in Fig. 3-a and b.

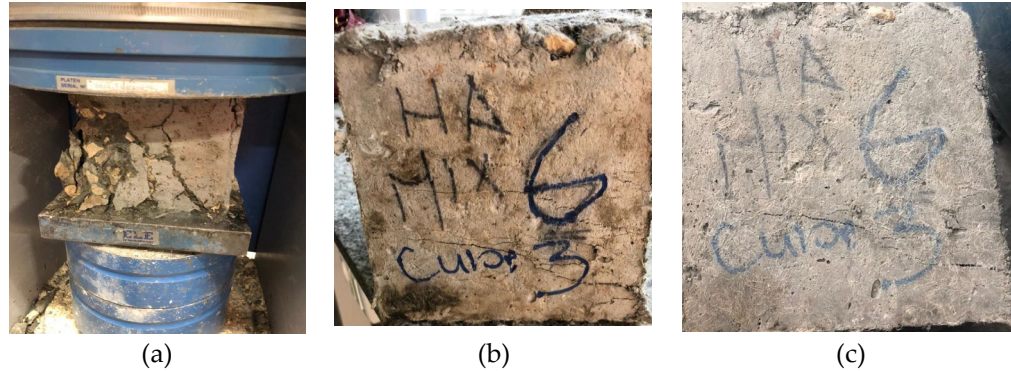


**Fig.3** Typical cube specimen (a) after failure (control/un-damaged specimen), (b) after pre-damaged by 60% of the ultimate capacity, and (c) after healing process exposure as per the age assigned for testing till crushing failure.

It should be mentioned that the values reported were averaged from the three specimens tested. As shown in Fig. 3-a, a typical control/un-damaged cube specimen was loaded till achieving failure load then a similar cube specimen was loaded till reaching the cracking load, as in Fig. 3-b. The cube specimen was cured by applying the healing scheme according to the assigned age and prepared for testing to failure, as shown in Fig. 3-c. It should be mentioned that the undamaged and pre-damaged cube specimens were tested for compressive strength as per BS EN 12390-3 [45] where the specimens were loaded at a pacing rate of 240 kg/cm<sup>2</sup> per minute till the specimen failure using the universal testing machine of capacity 2000 kN.

Similarly, the same loading scheme was followed for prism specimens to evaluate the flexural strength of the specimen, whether undamaged, pre-damaged, or after exposure to the healing scheme. The flexural test was handled for the control prism specimen to determine the peak load as per ASTM C78/C78M [46]. The specimens were tested on the flexural machine under two-point loading after adjusting a pacing rate of 24 kg/cm<sup>2</sup> per minute till failure. Following the similar scheme of cube specimens, the prism specimens were loaded till failure for control/un-damaged prism specimens, as shown in Fig. 4-a. 60 percent of the peak flexural load [47 - 49] or the corresponding load for the threshold crack width of 0.1 mm was applied to the pre-damaged the prism specimen, see Fig. 4-b. Thereafter, the specimens were left for curing as per the aging assigned for testing, as shown in Fig. 4-c.

The curing regime in which both cube or prism specimens are cyclic wet and dry. The curing process involves submerging the specimens into the water tank and drying them in the air at room temperature, inside the laboratory. The process was repeated successively at 24-hour intervals. This method simulates natural environmental moisture fluctuations that can trigger self-healing in cementitious materials as suggested by Yang et al. [50]. The strength recovery was calculated as the percentage increase in peak load from the post-cracking to the post-healing state. During testing, the crack behaviour under loading was

also observed. Additionally, surface cracks were observed before and after healing using a visual inspection to make sure that the cracks were sealed. It should be noted that before pre-damaging the cube or prism specimens, the specimens were water-cured until they reached the age assigned for pre-damaging.



**Fig. 4.** Typical prism specimen (a) after failure, (b) after pre-damaged by 60% of the ultimate capacity, and (c) after healing process exposure as per the age assigned for testing till failure.

## 4. Experimental Results and Discussion

### 4.1 Slump

The slump was tested after putting all the concrete ingredients and mixing them to determine the workability of the concrete after adding PVA fiber or the bacteria as per the mix design. The results showed that the addition of both would reduce workability to a high level. The mix OC, which represents the control provided a slump of 10 cm. However, when adding the bacteria, as in mix BC, the slump reached 0.7 cm which means that the reduction has reached 93% while the slump was reduced more than that by 95% when adding a VF of 1% PVA fiber as in mix PVAC1. The slump for mix PVAC1 was 0.5 cm. Similarly, mixes PVAC1.5 and PVAC2 were reduced by 97 and 98% when the VF of the PVA fiber added was 1.5 and 2%. When combining both bacteria and PVA fiber (mix BC+PVAC1), the slump reached 0 cm which is a total reduction of 100%. From the results, the slump is influenced by the addition of bacteria and PVA fiber although the replacement of fly ash with cement should enhance the workability. However, fly ash did not counteract the negative impact caused by the bacteria and PVA fiber interactions between additives that dilute cement paste continuity. The spherical surface of fly ash would be the reason for improving the workability or reducing water which was already considered while designing.

Topića et al. [51] have studied the influence of PVA on cement paste in terms of fresh and hardened properties. The results of the flow test revealed that increasing the addition of PVA reduces the slump and workability as agreed with the investigation carried out herein. Topića et al. [51] suggested that this was due to the viscosity accompanied by the PVA fibers which cause mixing and pouring problems. Hence, increasing the PVA content would increase this viscosity and reduce the slump. Nevertheless, Topića et al. [51] suggested a hypothesis that required further investigation related to the relationship between the initial and final setting time delay that occurs when using the PVA fiber and hydration process. With their observation of setting times while flow and fresh state it was hypothetically assumed that there might be an unusual bump resulting from the restored unhydrated  $C_3A$  restored by the PVA barrier around the cement grains. These restored hydrated particles of



C<sub>3</sub>A produce ettringite and thus increase the diffusion of the water to complete the hydration of C<sub>3</sub>A. Another aspect would be the bacteria itself which also showed a reduction in the workability of the mixture BC and BC+PVAC1. This could be attributed to the absorption of the bacteria for more water to deposit layers of CaCO<sub>3</sub> into the cavities, pores, and micro-cracks of concrete [52]. Hence, their hydrophilic nature would reduce the water content within the mix. Similar findings were deduced by Zhang et al. [53]. Their results provided that the PVA fibers addition in cementitious composite decreased its workability.

The workability reduction increased from 60 to 30 mm with increasing the PVA volume fraction (0.3–1.2%). Zhang et al. [53] attributed this behaviour to the creation of a network structure by the PVA fibers within the cementitious composite. This action restrained segregation and workability from being possessed. Further, they assumed that some cement particles might be absorbed onto the fiber surfaces and wrapped the fibers around. This behaviour would reduce the effective paste to contribute to the mixture's workability. It should be noted that Zhang et al. [53] added a water reducer to their cementitious mixture which was not countable here in this study as might influence the bacteria environment that was not clarified in any existing literature review. On the other hand, Safiuddin et al. [54] ensured that the bacteria would increase the workability and the enhancement may reach 45% higher than that of the control mix at high bacteria dosage. This was different from the findings attained here in this study as the slump was reduced when using the bacteria (mix BC). It should be mentioned that similar bacteria in Safiuddin et al. [54] investigation used; the bacteria *Bacillus subtilis*. Although the enhancement observed by Safiuddin et al. [54], stated that the bacteria activated once it encountered water, feeding on calcium lactate and growing to self-heal the cracks at 48 hours increased to 72 hours at high bacteria dosage. This action contradicted the slump results as this observation would absorb the water from the fresh state. This is simply because the bacteria dosage was added at the mixing stage without incorporating it within capsules. Further, an investigation is required in this area for more clarification and demonstration of the influence of the bacteria on self-healing.

Hence, the findings confirm the need to use superplasticizers when using bacteria and PVA fiber after exploring the influence of the superplasticizer on the performance of bacteria and PVA fiber in the healing process of concrete. Superplasticizers achieve this through their dispersive properties through electrostatic repulsion as dominant [55]. Flatt et al. [55] stated that the superplasticizers in their basic forms such as sulfonated formaldehyde condensate (SNFC), lignosulfonates, or salts of polycarboxylic acids (PCA) require specified calculations related to steric repulsion. This dispersive effect increases the fluidity of the cement paste, making it easier to uniformly disperse the hydrated cement, bacteria, and fibers throughout the mix [52, 54]. Thus, such behaviour could counterbalance the water-demanding nature of bacteria and the viscosifying effects of fibers, lubricating the concrete matrix, untangling clumps, and preventing re-agglomeration during mixing. The enhanced dispersion allows bacteria and fibers to be more equally coated by a hydrated cement paste, reducing frictional interactions that enhance the workability. Hussein et al. [52] have examined the suitable dosage of superplasticizer in their cementitious mixture through different percentiles. They found that as the superplasticizer increased the reduction of water content would reduce reaching 35% at 2.5 liters to each 100 kg cement and reducing the water ratio from 0.42 to 0.27.

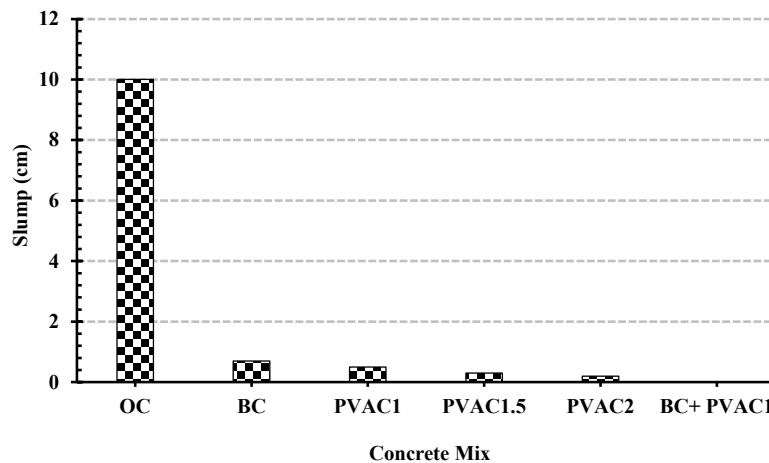


Fig. 5. Slump results for all mixes before hardening state properties.

## 4.2 Density

The density of all mixes was measured from the cube specimens in their hardened state before implementing any healing process or pre-damaging to the cube specimen at 28 days of age. As shown in Fig. 6, the density at 28 days of age after hardening decreased slightly with the addition of PVA fiber. The density is an important aspect as it forecasts compressive strength and shows the possibility of the presence of pores or not as the relationship between the density and compressive strength is proportional [56]. In other words, as the density of the concrete mixture increases the compressive strength increases [56]. Nevertheless, very few researchers addressed the influence of adding PVA onto the mortar or concrete mixture. However, most of those exploring the self-healing techniques using the fly ash as partial cement replacement and PVA fiber did not investigate the density of the mixture produced either before or after the implementation of the healing process as scanned through the existing literature review [21, 22]. It is anticipated that the fiber would increase voids based on the investigation carried out by Topič et al. [51]. They reported that the addition of PVA into the cementitious matrix has increased the porosity and therefore reduced the density which in turn reduced the compressive strength of their mixture. This behaviour was observed using optical and electron microscopy images (SEM) [51].

Yew et al. [57] also explored the low volume fraction of PVA in a cement matrix and found that the PVA attains lower density in both light weight and normal concrete. They attributed this behaviour to lower specific gravity although Shafigh et al. [58] reported that steel fibers which is the most used fiber for improving the mechanical properties of concrete. Their results, contrary to the PVA fiber, revealed that increasing the volume fraction of steel fibers would increase the density of the concrete. Hence, Yew et al. [57] confirm that the low specific gravity would be the main reason for the slight reduction in density while increasing the PVA fiber volume fraction. However, when exposed to their concrete to preheating, the results revealed that PVA fiber tends to displace mortar in concrete. From Fig. 6, the mixes already included the bacteria besides the PVA fibers at different percentiles. As clear, the reduction in density is relevant to the addition of PVA fiber which agrees with the findings of Topič et al. [51] and Yew et al. [57]. As the PVA fiber percentile

increases the density decreases due to the lower specific gravity which is near to one as addressed in Table 3.

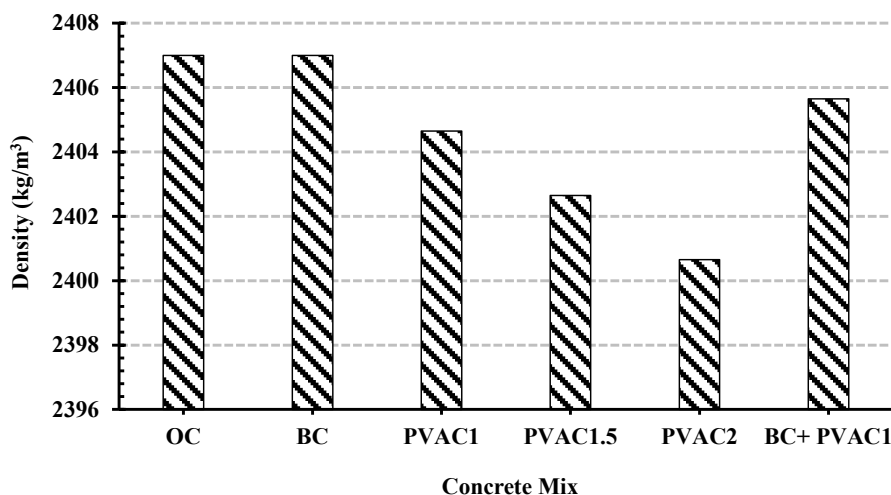


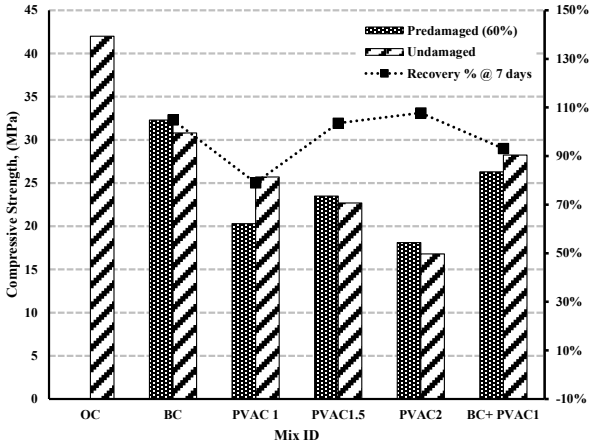
Fig. 6. Density results for all mixes at 28 days of age after hardening state properties before initiating cracks or applying the healing process.

### 4.3 Compressive strength

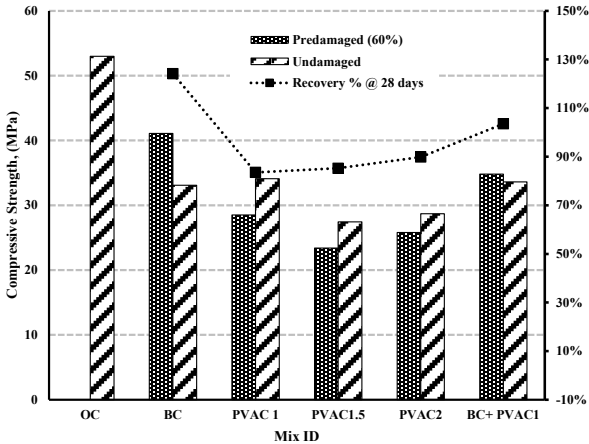
Compressive strength is a very important aspect of any structural element as concrete can handle compression stresses more than tensile ones. Thus, concrete deterioration and degradation of strength is a crucial issue. The healing and recovery of strength could provide a new era in concrete technology especially when it comes to the repair and maintenance of structures and their operation. Self-healing in this case could be an alternative even though the capital of investment would be high at the beginning. From Fig. 7, both techniques of self-healing enhanced and improved the concrete strength after being cracked. The figure shows gained strength through the ages while initiating cracking through pre-damaged specimens and the recovery gained after applying the healing process of a wet and dry cycle for each mix with a period according to their ages except for 7 days of age, the healing process of cycles wet and dry was applied for 28 days only. The initiation of cracking took place after testing three specimens till failure (un-damaged) and the damaged specimens were created for each mix by applying 60% of its capacity to initiate the crack width of more than 0.1 mm. Fig. 8 shows the crack initiation of the cube specimens before and after encountering the healing process.

Usually, the influence of the healing process can be evaluated through the crack closure, as shown in Fig.8, and the compressive strength recovery was plotted as presented in Fig. 7 [59]. Zhang et al. [59] stated that the concrete itself cannot heal on its own as the hydration reaction of cement particles and the crystallinity of additives is unable to close cracks of this size. The evidence was deduced when leaving the initiated cracked cube specimen after 28 days of curing at room temperature. On the other hand, the self-healing granules provided closure for the crack as stated by Zhang et al.[59] where their results revealed that at 7 days of curing 0.963 mm would be repaired in just 7 days. However, it should be mentioned that

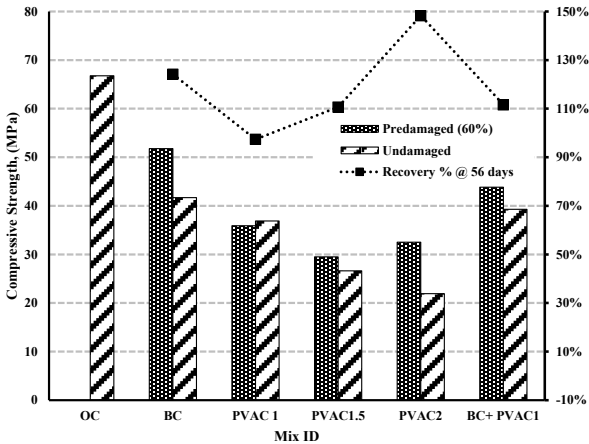
555 the faster healing process is dependent on the types of healing material used whether it is  
556 bacteria or chemical additives.



(a) 7 days\*



(b) 28 days



(c) 56 days

\*The 7 days of age curing was then encountered in the healing process (dry and wet cycle) for 28 days

557 Fig. 7. Compressive strength results for the cube specimens for all mixes after hardening  
558 with (pre-damaged) and without (undamaged) applying the healing process at (a) 7, (b) 28,  
559 and (c) 56 days of age.

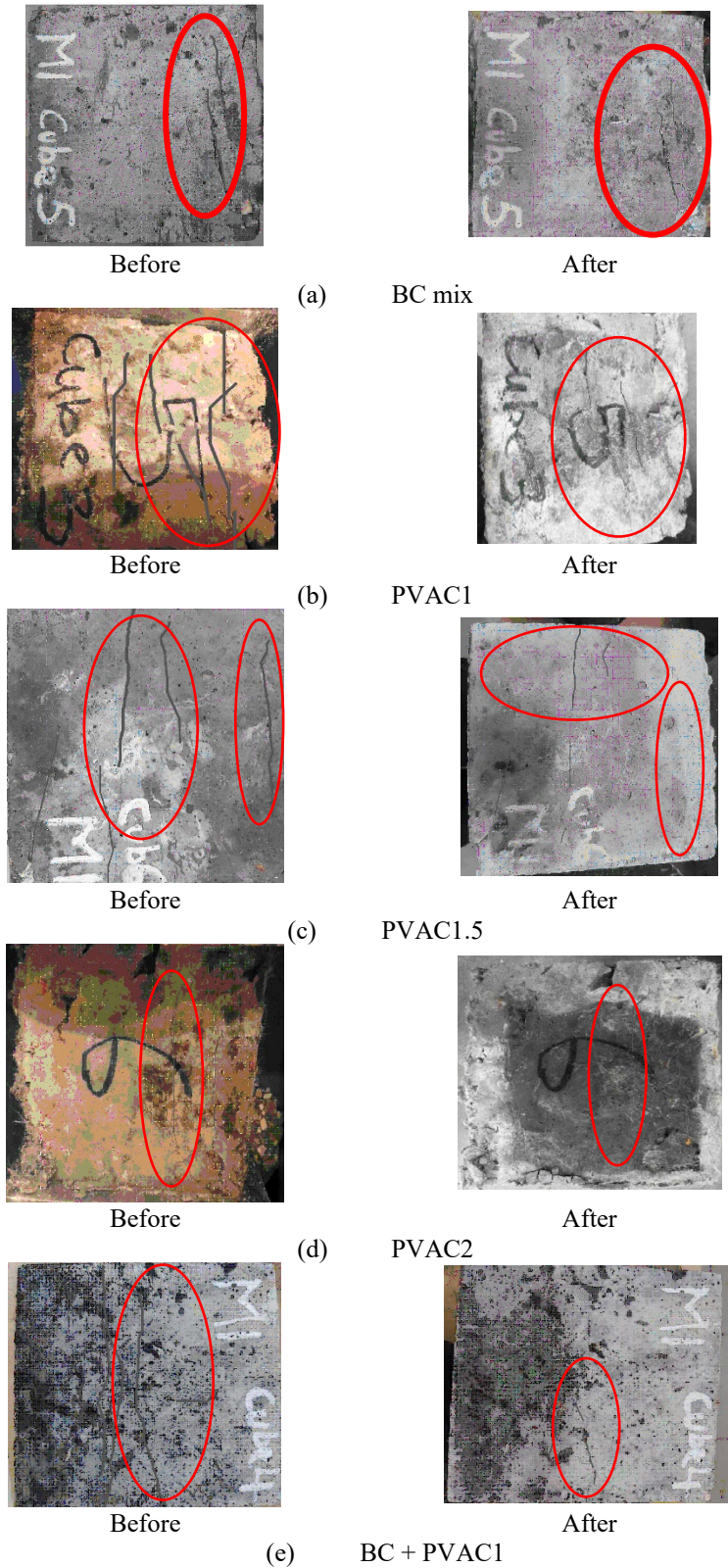




Fig. 8. Crack closure of cube specimens at initiating cracks and after applying the healing process at 28 days of age for mix (a) BC, (b) PVAC1, (c) PVAC1.5, (d) PVAC2, and (e) BC + PVAC1

In Zhang's study, the materials were self-healing granules, which require no temperature or chemical activation and the inner core of the inorganic mineral of these granules provides good compatibility and long-term stability with cement-based materials [79]. Nevertheless, the healing bacteria used and PVA fiber including the use of fly as mineral additives helped in healing the concrete, as shown in Fig.8. Compared with the control mix, it is clear from Fig. 7-a, b, and c, that the undamaged specimens attain a value of 73, 62 and 62% for mix BC of that of the control mix at 7, 28 and 56 days of age. Similarly, the mixes PVAC1, PVAC1.5, and PVAC2 revealed a compressive strength for the undamaged cube specimen of 61, 64, 55, 54, 40, 40, 54, and 33% at 7, 28 and 56 days of age, respectively. while the compressive strength of undamaged cube specimens for mix BC+PVAC1 showed values of 67, 63, and 59% of that of the control mix, at 7, 28, and 56 days, respectively. It should be noticed that the crack widths were not measured as the crack pattern was different than the flexural, as shown in Fig.8.

From Fig.7, the compressive strength of cube specimens for BC mix at 7 days has a recovery of 105% after the healing process. While those with added PVA fiber at 1, 1.5, and 2% the recovery at 7 days were 79, 104, and 108%, respectively for mix PVAC1, PVAC1.5, and PVAC2. The mix BC + PVA 1 was recovered by 93%. Thus, the PVAC2 provided the highest compressive strength recovery which is attributed to the lower compressive strength of the un-damaged cube specimens due to the high PVA volume fraction. This high volume fraction of PVA fiber increased the porosity, which in turn lowered the compressive strength. Also, it should be mentioned that the OC mix might have provided a greater grade at failure stress than other mixes with BC and PVA addition at 7 days of age.

At 28 days, the recovery revealed a different trend than that of 7 days. The mix BC provided a strength recovery of 124 %, while the mix PVAC1, 1.5, and 2 provided a recovery of 84, 85, and 90%, respectively. Finally, the mix BC + PVAC1 showed a strength recovery of 104%.

At 56 days, the recovery revealed a similar trend with lower gaining strength. The mix BC revealed a strength recovery of 124%, while the mix PVAC1, 1.5, and 2 retained a strength of 97, 111, and 148%, respectively. However, the mix BC + PVAC1 showed a strength recovery of 112% which is between that of mix BC and mix PVAC1 individually. The mix BC and PVAC2 showed improvement relative to those with mix BC + PVAC1. The reason for the improvement in general along with those of coupled effect was explained by demonstrating the mechanism of using bacteria or PVA fiber or utilizing both combines. In general, lowering the PVA fiber would reduce the porosity and therefore would increase the compressive strength. As clarified earlier through ages, the un-damaged cube specimens for mix PVAC1 were relatively higher than those of the mix PVAC2, which confirms the existence of more voids and lower density [51, 56, 57] as explained earlier in section 4.2. this behaviour would, in turn, reduce the compressive strength of the concrete mixture regardless of the bridging provided by the PVA fibers and the precipitation of high calcium carbonate that would enhance the concrete performance and fill the voids as explained in the next few lines through the studies reported by Feng et al. [21] and Qiu et al. [22].

The mechanism of both bacteria and PVA fiber was reported by Feng et al. [21]. Feng et al. [21] observed the presence of a high concentration of nutrients and some intermediate metabolite or inducible enzyme in inoculated bacterial solution. The growth rate of the bacteria decreased with the greater consumption of intermediate metabolite and hence induced enzymes could be developed through the anabolic process of bacteria. The reduction in the growth rate of bacteria was measured by breeding speed and the death rate occurred through metabolite accumulation. However, the results revealed that calcium carbonate possessed in a solution even with different fiber types was all calcite. Nevertheless, both PP and PVA fiber showed no significant influence on the components of products induced by bacteria [21]. Through their XRD, it could be observed that an increase in peak intensity occurs with the inclusion of fiber into the solution and PVA showed higher angles which implies the formation of larger and smaller crystallites [21]. Through their investigation, the particle size was measured to evaluate the volume fraction of calcium carbonate precipitation by PVA fiber, which showed a higher amount of larger particle size of calcium carbonate precipitation. In other words, the PVA presence did not influence the polymorph of calcium carbonate induced by bacteria, but PVA fiber increased the particle size of calcium carbonate [21].

The coupled effect of PVA fiber and bacteria was observed when Feng et al. [21] observed white crystals precipitated on the fiber surface of the specimens containing BC and PVA fiber more than those of PVA fiber only. The main elements of the precipitation were C, O, and Ca, confirming the deposition particles were calcium carbonate. In addition, microbial-induced calcium carbonate absorbed on the surface of cracks was observed. They attributed that the contribution of PVA would be due to the high polarity strength in their molecular structures which easily attract the calcium ions and promote the formation of calcium carbonate, in addition to, their analysis of the cell parameter which provided close results to those of calcite which means that the hydroxyl groups of crystalline PVA are almost equal to that calcium ion of aragonite, generating aragonite requires a large number of magnesium ions or special proteins that are rare inside the paste matrix [21]. Hence, both bacteria and PVA possess nucleation sites for calcium carbonate, inducing calcium carbonate precipitation, which was explained by the high utilization of calcium ions in specimens including bacteria and PVA fiber, in addition to, the difference in particle size for calcite generated in solution for mixes including PVA fiber than those with bacteria only.

On the other hand, Qiu et al. [22] observed the mechanism of PVA fiber with other mineral admixtures such as the slag, and deduced that the healing products, distinct from the matrix, grew in the crack and almost filled the 100  $\mu\text{m}$  gap. The healing products are composed of irregularly precipitated crystal-like particles. While the large particles ( $\geq 10\mu\text{m}$ ) fill the major portion of the gap, smaller particles ( $\leq 10\mu\text{m}$ ) can be found in the void between the large particles and the crack surface. the crystal-like particles grow from very small precipitates, several hundreds of nanometers in size, and precipitate on the PVA fiber. Fiber bridging might very likely facilitate the precipitation of healing products and promote healing in Engineering cementitious concrete (ECC). Through the EDX, the healing products composition was identified and were as follows; calcium, silicon, and carbon possess the presence of  $\text{CaCO}_3$  and/or C-S-H as the main products, in addition, the Ca/Si ratio of the healing products for the samples was in the range of 5.63 to 7.18, which nearly agrees with Feng et al. [21] findings. The possession of free  $\text{Ca}^{2+}$  ions and their



concentration is related to the  $\text{Ca}(\text{OH})_2$  dissolved and the alkalinity of the pore solution in the matrix, which in turn produces more  $\text{CaCO}_3$  which is considered the main dominant healing product in samples.

The crack closure results revealed also unique trends based on Fig.8. Mixes BC, PVAC2, and BC + PVAC1 showed the maximum crack closure and the disappearance of crack propagation onto the surface of the cube specimens as shown in Fig. 8-a, b, and e. Similarly, the mixes PVAC1 and PVAC1.5 showed the healing of some cracks but in lower number and width than that of the other mixes. Cracks with a maximum width of 0.3 mm are not visible for all the specimens. This suggests that the self-healing bacteria and PVA fibers along with the addition of fly ash as mineral admixtures have deposited the chemical reaction form of calcium bicarbonate causing physical and chemical reactions to bond and seal the cracks. These results agree with the findings of Feng et al. [21] and Qiu et al. [22]. Their result confirms the coupling effect of using bacteria and PVA, in addition to their benefit to the crack healing process. Hence, the closure of the crack width would in turn reduce the porosities and regain the compressive strength of the concrete mixture.

#### 4.4 Flexural strength

Similar to compressive strength and more crucial is flexural strength as most of the concrete structure elements are subjected to bending moments which generate tension on concrete causing cracking. Fig. 9 shows the results of the pre-damaged and undamaged prism specimens for flexural at 7, 28, and 56 days of age. It should be mentioned that the curing methods adopted as per the age of testing expect for 7 days the healing process took around 28 days of age after pre-damaging the specimens.

Compared with the control mix, it is clear from Fig. 9-a, b, and c, that the undamaged specimens attain a value of 73, 61, 54, 40, and 67% for mixes BC, PVAC1, PVAC1.5, PVAC2, and BC+PVAC1 of that of the control mix at 7 days of age. Similarly, at 28 days of age, the undamaged cube specimen for mixes BC, PVAC1, PVAC1.5, PVAC2, and BC+PVAC1 revealed a value of 62, 64, 52, 54, and 63%, respectively. Finally, the undamaged cube specimen at 56 days of age provided a value of 62, 55, 40, 33, and 59% of that of control for mixes BC, PVAC1, PVAC1.5, PVAC2, and BC+PVAC1, respectively.

Feng et al. [21] explored the repaired area in prism specimens for those with bacteria and PVA fibers and with coupled inclusion through a prism specimen tested in bending to create mid-crack. The exploration was performed by stereo microscopic and binarization images of crack surfaces to measure the crack width and the repaired area. In general, their results revealed that the control specimens retained 31% on average of their crack repaired after 7 and 28 days of age which was attributed to the continuous hydration of cement paste carried out in the crack inner surfaces and carbonization reaction. However, the prism specimens with PVA fibers achieved about 44 to 50 % at 7 and 28 days of age indicating the improvement of the healing process using the PVA fibers. In the current study, the crack width was measured as shown in Fig. 10. The crack width closure reached nearly 95% of

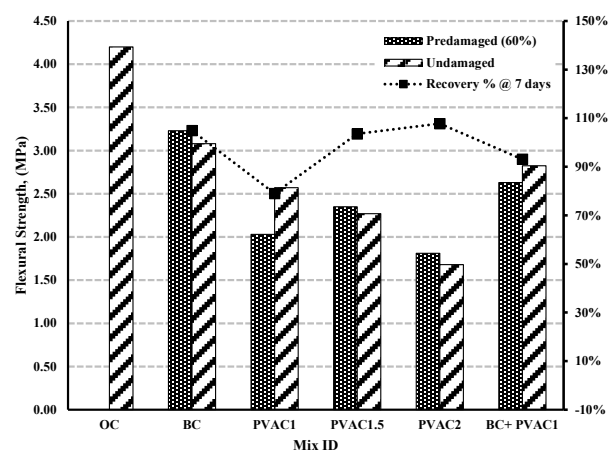
that of the original crack width. Similar findings were found in the literature [14, 22, 61] that the PVA fibers provided the most reliable healing and recovery enhancement among the other fibers (i.e., PP fiber, etc.). Feng et al. [21] also reported that the mixtures with bacteria provided more repaired areas achieving over 50 and 74 % of the cracked area after 7 and 28 days of implementing the healing process. These findings were similar to those observed by Luo et al. [61].

From Fig.9, the flexural strength of prism specimens for BC mix gains strength recovery of 105, 124, and 124% after the healing at 7, 28, and 56 days of age. While those with added PVA fiber at 1, 1.5, and 2% the recovery at 7 days were 79, 84, 97, 104, 85, 111, 108, 90, and 148%, respectively for mix PVAC1, PVAC1.5, and PVAC2 at 7, 28 and 56 days of age.

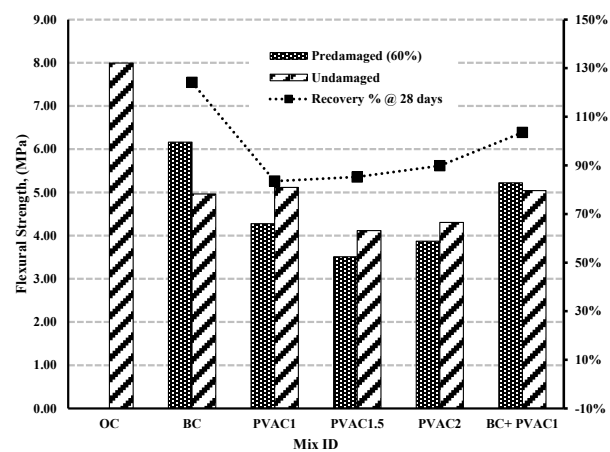
Feng et al. [21] also observed the coupling of the effect through the mortars with a combination of PVA fiber and bacteria which attain a higher healing area of the cracks for the prism specimens than those with PVA fibers only, reaching 55.2% and 64.6% at 7 and 28 days of age. Nevertheless, their observation showed lower values of repaired area for cracks in prism specimens than those with bacteria only. Their reasons were around two main aspects; one was that bacteria induced more calcium carbonate into those mixes with fibers and the second was the fiber attracted some calcium ions dissolved and captured on the fiber surface deposited within the inner crack surface which in turn inhibited the bacteria activity and produced lower calcium carbonate concentration on the inner crack surface than those mixes with bacteria only. This behaviour would be ascribed to the larger particle size of calcium carbonate possesses by the PVA fibers in addition to the absorption property which the PVA fiber might utilize in absorbing more bacteria accelerating the precipitation of carbon dioxide on the crack surface and initiating the generation of calcium carbonate.

The mechanism was discussed by several researchers [21, 62 – 64, 65]. For instance, Feng et al. [21] studied the prism specimen under bending as stated earlier, and showed the results provided un-damaged and cracked specimens. In general, all of the specimens with bacteria, PVA fibers, or a combination of both showed lower flexural values than those of the control which agrees with the current study. They attributed that the bacteria medium would have encountered an adverse influence on the flexural capacity of the mixtures. This behaviour was observed by the uneven distribution and volume expansion initiated by the calcium carbonate inclusion resulting in microcracks in the carbonated zone [62 – 64]. Similarly, the PVA fiber mixture provided some voids due to the volume fraction, and thus, the same observation was denoted for the mixture with both bacteria and PVA fiber in which the flexural strength of the prism specimens is lower than that of the control. The behaviour as clarified earlier is similar to the result attained in the current study; however, there was no opportunity to measure the cracking area using stereo microscopic and binarization images of crack surfaces. Nonetheless, the PVA fiber cracked/pre-damaged specimens attain the role of stress transferring crossing the cracks in a bridging manner while preventing crack propagation which influences the flexural strength capacity relevant to the

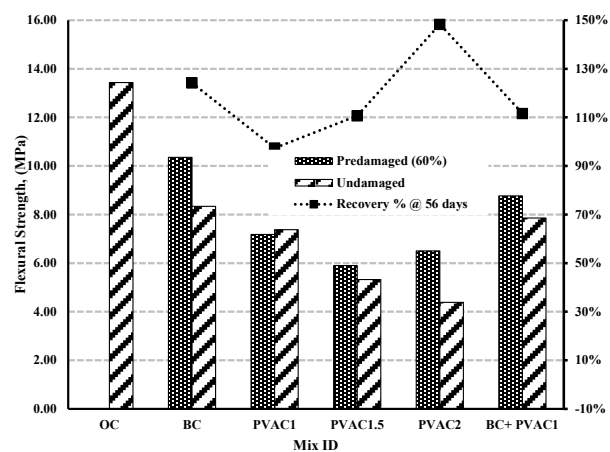
729 cracked/pre-damaged specimens with bacteria and combined; bacteria and PVA after  
 730 implying wet/dry cycle regime [65].



(a) 7 days\*



(b) 28 days



(c) 56 days

\*The 7 days of age curing was then encountered in the healing process (dry and wet cycle) for 28 days

Fig. 9. Flexural strength results for the prism specimens for all mixes after hardening with (pre-damaged) and without (undamaged) applying the healing process at (a) 7, (b) 28, and (c) 56 days of age.

However, the mixes with bacteria and PVA fiber provided a lower flexural strength compared to those of PVA fiber only. Flexural recovery attained by mixes with PVA1 fiber and bacteria was 23%, which was slightly lower than that for specimens with PVA1 fiber only (24%). Thus, it was concluded that fiber addition played a vital role in flexural recovery, especially with crack widths reaching  $0.4 \pm 0.1$  mm. Similar results were deduced when investigating the coupling effect of bacteria and PVA fiber which proved an insignificant influence on the flexural regain [66]. This was relevant to the surface mineralization treatment with calcium carbonate [66] and the precipitation amount on PVA fiber surfaces, concluding better performance to those of PVA fiber than those of bacteria and PVA fiber combined. Further, Chen et al. [67] reported that immobilizing the bacteria could retain 72% of the flexural recovery while 50 to 80% when adding fibers [68].

In conclusion, selecting the carrier for products possessed by bacteria would result in enhancing the flexural regain of the cracked mixture, hence, the coupling influence of bacteria and PVA fiber was observed in the high crack area closure rate.



Fig. 10. Crack closure of prism specimens at initiating cracks and after applying the healing process at 28 days of age for mix BC + PVAC1

The mix BC + PVAC1 was recovered by 93, 104, and 112% at 7, 28, and 56 days of age. Thus, the BC + PVAC1 provided the highest compressive strength recovery. It should be mentioned that the OC mix might have provided a greater grade at failure stress than other mixes with BC and PVA addition at 7 days of age. Due to the difficulty in measuring and getting more photos for the flexural prism specimens before and after the healing process, only mix BC+PVAC is presented, as shown in Fig.10. The figure shows the closure of the crack of 0.3865 mm after 28 days of curing exposed to wet and dry cycle have reached to 0.0714 which means that nearly 95% of the crack width was closed and filled with PVA and the bacterial reaction that possessed more calcites as illustrated by Zhang et al. [59].

It should be noted that Shaaban et al. [69] revealed similar results in terms of compressive and flexural strength for the bacterial mix; Mix BC as their results provided a

high gain in strengths when using *B. subtilis* at  $10^8$  cells/ml, not  $10^5$  cells/ml as per their investigation and experimental program which is similar to the findings in both compressive and flexural strengths revealed here in this study.

#### 4.5 Absorption Percentile

Absorption is one term that can determine and evaluate the durability of concrete. An average of three cube specimens was reported. The test surfaces should be at the same distance as the exposed distance from the original exposed surface of the concrete. Then, the specimens should be handled in an environmental chamber at a temperature of  $50^\circ\text{C}$  and relative humidity of 80% for three days and then sealed in that specimen. The specimens are arranged with a space to allow for airflow in between and stored at room temperature.

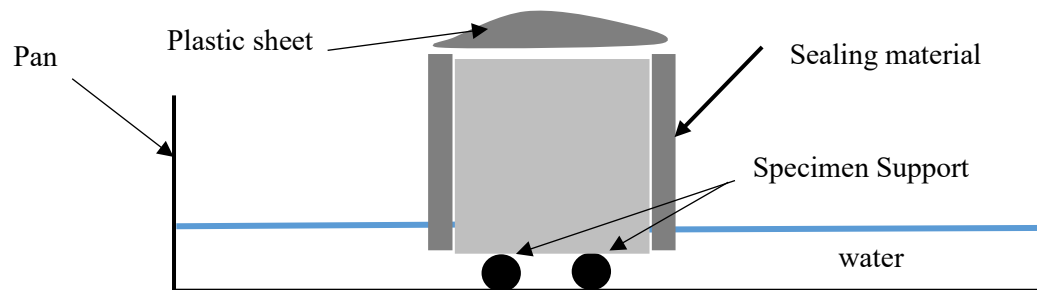


Fig. 11. A typical cube specimen under absorption testing

After a minimum of 15 days, the specimens were vacuumed while sealing the end face with plastic sheets using a vacuum pump for 3 hours and exposing it to tap water through the vacuum chamber. The specimens were soaked for 18 hours underwater and then weighed the specimen. The side surface and one end that is not exposed to water were sealed with a plastic sheet that can be secured using an elastic band. The initial mass was weighed and then specimens were placed into tap water with a height of 3 mm using supports. Then the specimens were weighted at several intervals of time [41], as shown in Fig. 11.

The records are then plotted and presented, as shown in Fig. 12. Absorption rate for the bacterial mix showed the lowest values among all the mixes which means that the bacteria possessed a reaction that would increase the existence of more calcite closing all the pores inside the concrete or at least the network between pores would be closed. On the other hand, the mixes PVAC1, PVAC1.5, and PVAC2 which contain PVA fibers would have a higher absorption rate than the other mixes including the control "OC". This is attributed to the absorption rate of the fiber itself stated by Jain et al.[70], Shen et al.[71], and Li et al.[72]. They stated that the PVA fibers have a high intake of water and can reach 41.97 % moisture adsorption content at 8 hours of water exposure. They confirmed that the outer pure PVA tissue would get saturated for longer water exposure of water. Nevertheless, adding the bacteria with the lowest percentile of PVA (1%) as in mixBC+PVAC1 the absorption rate would be reduced reaching a minimized value between those of mixes BC and PVAC1. It should be mentioned that mix PVAC1 showed the lowest among the mixes with PVA fibers as it contains the lowest volume fraction of 1% while the other contains 1.5% and 2%. From the results, it is very clear the effectiveness of using PVA fibers in healing the concrete.

On the other hand, Feng et al. [21] have measured both the absorption and sorptivity of the mixes. Their results revealed that the absorption with the control specimen was the highest among all the other mixes and the absorption rate reduced with time. Similarly the specimens for mix with bacteria but still lower compared to the control specimens. They attributed this reduction to the fact that the precipitated calcium carbonate is conducive to reducing water uptake on the surfaces and inner cracks induced by bacteria, in addition to, the swelling due to pore size reduction [73, 74]. The absorption for mixes with PVA fiber was lower than that of control since fiber could refine the pore structure by subdividing them into small pores [75], in contrast to the current results here in this study, in which the PVA fiber showed higher absorption due to the absorption property attained by the PVA fiber. Feng et al. [21] results confirmed that the fiber diameter influenced the absorption reduction the lower the diameter the higher the absorption reduction. This action was demonstrated by well-dispersed shorter fiber that could increase the tortuosity and roughness of cracks. This behaviour would in turn reduce the rate of water surpassing the cracks [76, 77]. Their results, also, revealed that the fiber provided more efficiency in improving the water tightness of cracked mortars than those of mixes with bacteria since the absorption rate of mixes with fiber showed lower values than those of bacteria. On the other hand, the mixes in which both bacteria and fiber provided lower absorption than those mixes with fiber or bacteria only. In conclusion, their investigation reported that the inclusion of both PVA fiber and bacteria efficiently enhanced the water tightness for healed cracks by sealing the voids and pores.

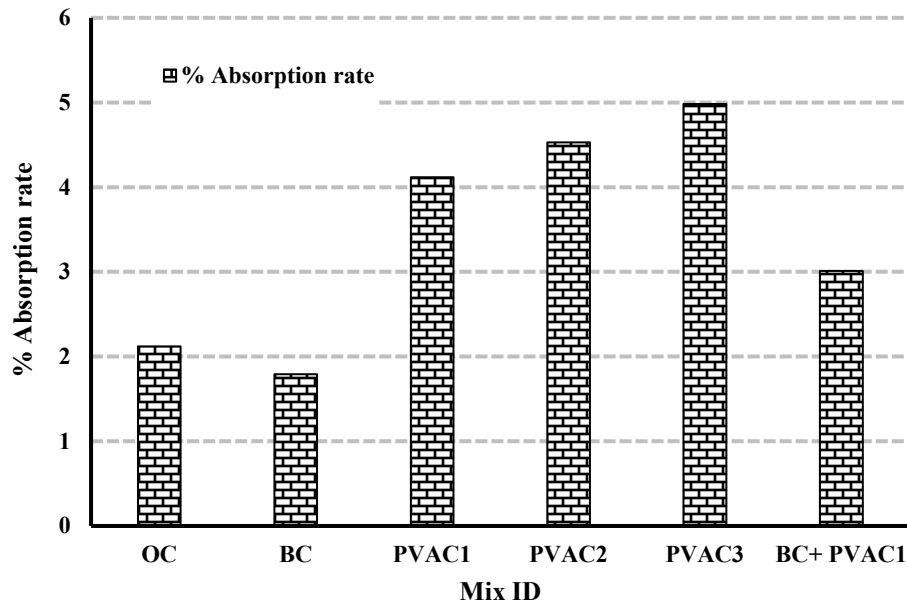


Fig. 12. Absorption rate of the mixes at 28 days

#### 4.6 Sorptivity

Sorptivity, or capillary suction, is the transport of liquids in porous solids due to surface tension acting in capillaries [78]. It is a function of the viscosity, density, and surface tension of the liquid, and the pore structure (radius, tortuosity, and continuity of capillaries) of the solid [78]. Sorptivity is a material's ability to absorb and transmit water through it via



capillary suction and provides an engineering measure of microstructure and properties important for durability[79]. Sorptivity is increasingly being used as a measure of concrete resistance to exposure to aggressive environments. The water sorptivity test is a unidirectional absorption test [79, 80]. Usually, the specimens are coated with epoxy from their sides and placed into water and  $\text{Ca}(\text{OH})_2$  to measure the suction rate of water using capillary conceptual. Fig. 13 shows the specimen under testing while pressuring the water for testing sorptivity and evaluation rate of absorption unidirectional using scaled grade as per ASTM C1585 [80] regulations.



Fig. 13. A typical cube specimen under sorptivity testing [79, 80]

Fig. 14 shows the depth value exposed to water because of suction capillary action for the cube specimen of each mix among the six mixes. The mixes showed a similar results trend to the absorption rate. The mix BC showed a lower suction rate as the pores mostly was closed by calcites [70]. The mixes with PVA fiber showed high suction rates especially those with high VF (2%) as in mix PVAC2. The addition of BC to the PVA fiber as in the mix BC+PVAC1 provided a suction rate nearly to that of mix BC which means that the bacteria have a high influence in reducing the absorption rate of the PVA fiber because of depositing more calcite onto the surface of PVA fibers [38].

Few researchers have studied the sorptivity [21, 22, 81, 82]. Feng et al. [21] explored the sorptivity of the cracked specimens after healing for 28 days and found similar trends to those of absorption results. On the other hand, un-damaged specimens for mixes with bacteria showed a higher rate of sorptivity than that of control samples. In other words, the bacteria inclusion provides lower water resistance than the control specimens since retarding effect occurred by sucrose [81, 82] in the bacterial medium.

However, mixes with bacteria or PVA fiber or both provided conversely, lower rates than that of control samples at reduction values below 50%, in contrast to 120% for the control specimens which means a significant increase in initial sorptivity coefficient for samples after cracking. Specimens with PVA1 fiber and bacteria showed lower sorptivity coefficient values than those of samples with PVA1 fiber or bacteria respectively. It indicated that the coupling effect of bacteria and PVA1 fiber could be conducive to an increased water resistance of mortars. Comparing results of area repair rate, capillary water absorption, and sorptivity reduction for self-healing, it could be inferred that more calcium carbonate precipitated in the inner instead of surfaces of cracks for specimens with fiber and bacteria compared to those specimens with bacteria only.



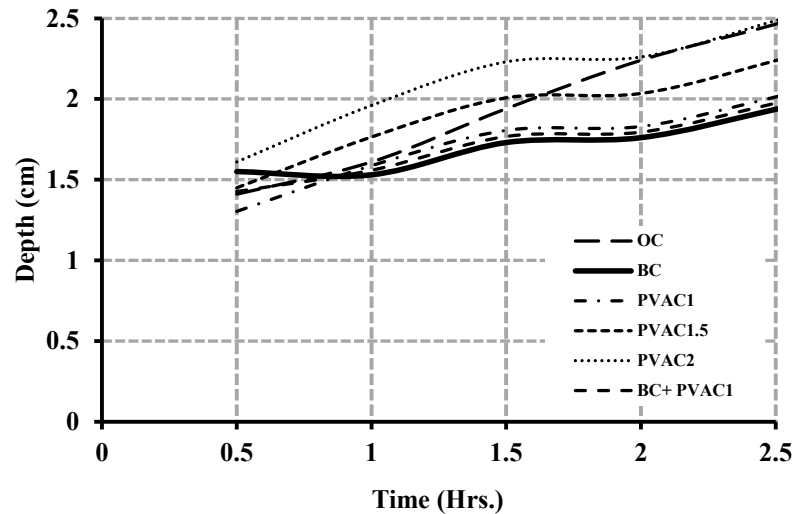


Fig. 14 Depth exposed to water

## 5. Conclusion and key findings

The study consisted of six mixes that were cast, including control mix, *B. subtilis* bacteria, and PVA fiber addition at various percentile (1, 1.5, and 2%). The sixth mix presented the coupling effect where the bacteria and the mixes with PVA fiber addition at VF of 1% were combined. Mechanical properties in terms of compressive and flexural strengths at 7, 28, and 56 days were evaluated after initiating cracks and the healing process applied. Furthermore, durability testing was carried out through absorption rate and sorptivity evaluation for the specimens after exposure to the healing process of wet and dry cycle curing at 28 days. The results provided in terms of mechanical properties and durability of concrete revealed that the coupling would provide optimized results between those using bacteria and PVA fiber addition. Nevertheless, bacteria production requires a very difficult process for cultivation and growth as well as serious precautions such as the environment of adding the bacteria in concrete would be damaged while mixing. However, the results showed the following:

In terms of fresh state properties, the addition of bacteria and PVA fibers reduced the workability, and it was recommended to use the superplasticizer in this case. Yet no researcher investigated the different types of waster-reducer based on the bacteria environment or their influence on the PVA fiber addition while being added with fly ash as a mineral admixture.

It was observed that the density revealed nearly similar values to that of the control; however, when adding the PVA fibers the density decreases due to the PVA fiber specific gravity and the lower density is due to the creation of more voids when using the PVA fibers.

The mechanical properties of both the comprehensive and flexural strength revealed a similar trend. The results revealed that the coupled effect would provide an optimized strength in between the PVA of 1% and Bacteria with a count of  $1.08 \times 10^8$  cells/ml, solution concentration of 600 nm/liter. The best performance was revealed with those of bacteria addition and resulted in enhanced strength compared with that obtained with the other

896 mixes; however, precautions should be taken during production. The second mix is one with  
897 a PVA addition of 2%; however, ball formation might be the reason for the reduction of its  
898 general grading from the very beginning as noticed when compared to the strength of  
899 conventional concrete. Nevertheless, it provides increased strength with age (56 days).

900 The durability evaluation of concrete in terms of sorptivity and absorption rate indicated  
901 the influence of the bacteria was better than that of PVA fiber addition. The durable concrete  
902 should have lower sorptivity and low rate of absorption; however, due to the PVA fiber  
903 behaviour for the intake of water, both the sorptivity and the absorption rate were affected.  
904 The addition of bacteria, on the other hand, lowered the sorptivity instead along the cycle  
905 period.

906 Further investigation is required to study the techniques on an individual and coupled  
907 basis for further implementation of techniques in repairing the deteriorated concrete  
908 structures and how it would deal with the corroded steel reinforcement on short and long-  
909 term behaviour

910 In summary, the key findings from the investigation are as follows:

911 The bacterial self-healing mechanism facilitates pore closure in the concrete matrix by  
912 precipitating calcite crystals that grow and spread from nucleation sites on the bacterial cell  
913 walls.

914 This crystallization process progressively seals pores and cracks, reducing pathways for  
915 moisture ingress.

916 The coupling effect, consisting of combining the bacteria and the mixes with PVA fiber  
917 addition at VF of 1%, provides optimized results between those using bacteria and PVA  
918 fiber addition.

919 In terms of fresh state properties, the addition of bacteria and PVA fibers reduced the  
920 workability, and it was recommended to use the superplasticizer in this case.

921 With regards to the durability of the concrete in terms of sorptivity and absorption rate,  
922 the addition of bacteria has a more positive impact than that of the PVA fibers.

## 923 Compliance with Ethical Standards

- 924 - The authors declare that they have no conflict of interest.
- 925 - This article does not contain any studies with human participants or animals performed  
926 by any of the authors.
- 927 - The authors declare that they have no known competing financial interests or personal  
928 relationships that could have appeared to influence the work reported in this paper.

## 929 References

930 [1] Mihashi, H., & Nishiwaki, T. (2012). Development of Engineered Self-Healing and Self-  
931 Repairing Concrete-State-of-the-Art Report. In Journal of Advanced Concrete  
932 Technology (Vol. 10, Issue 5, pp. 170–184). Japan Concrete Institute.  
933 <https://doi.org/10.3151/jact.10.170>

934 [2] Nishiwaki, T., Kwon, S., Homma, D., Yamada, M., & Mihashi, H. (2014). Self-Healing  
935 Capability of Fiber-Reinforced Cementitious Composites for Recovery of Watertightness

and Mechanical Properties. In *Materials* (Vol. 7, Issue 3, pp. 2141–2154). MDPI AG. <https://doi.org/10.3390/ma7032141>

[3] Van Tittelboom, K., & De Belie, N. (2013). Self-Healing in Cementitious Materials—A Review. In *Materials* (Vol. 6, Issue 6, pp. 2182–2217). MDPI AG. <https://doi.org/10.3390/ma6062182>

[4] Roig-Flores, M., Formagini, S., & Serna, P. (2021). Self-healing concrete-What Is it Good For? In *Materiales de Construcción* (Vol. 71, Issue 341, p. e237). Editorial CSIC. <https://doi.org/10.3989/mc.2021.07320>

[5] C. Edvardsen, “Water Permeability and Autogenous Healing of Cracks in Concrete. (1999). In *ACI Materials Journal* (Vol. 96, Issue 4). American Concrete Institute. <https://doi.org/10.14359/645>

[6] De Belie, N., Gruyaert, E., Al-Tabbaa, A., Antonaci, P., Baera, C., Bajare, D., Darquennes, A., Davies, R., Ferrara, L., Jefferson, T., Litina, C., Miljevic, B., Otlewska, A., Ranogajec, J., Roig-Flores, M., Paine, K., Lukowski, P., Serna, P., Tulliani, J., ... Jonkers, H. M. (2018). A Review of Self-Healing Concrete for Damage Management of Structures. In *Advanced Materials Interfaces* (Vol. 5, Issue 17). Wiley. <https://doi.org/10.1002/admi.201800074>

[7] Wiktor, V., & Jonkers, H. M. (2011). Quantification of crack-healing in novel bacteria-based self-healing concrete. In *Cement and Concrete Composites* (Vol. 33, Issue 7, pp. 763–770). Elsevier BV. <https://doi.org/10.1016/j.cemconcomp.2011.03.012>

[8] Nishiwaki, T., Mihashi, H., Jang, B.-K., & Miura, K. (2006). Development of a Self-Healing System for Concrete with Selective Heating around Crack. In *Journal of Advanced Concrete Technology* (Vol. 4, Issue 2, pp. 267–275). Japan Concrete Institute. <https://doi.org/10.3151/jact.4.267>

[9] Nishiwaki, T., Mihashi, H., & Okuhara, Y. (2010). Fundamental study on self-repairing concrete using a selective heating device. In *Concrete Under Severe Conditions, Two Volume Set* (pp. 919–926). CRC Press. <https://doi.org/10.1201/b10552-116>

[10] Dry, C. M. (2000). Three designs for the internal release of sealants, adhesives, and waterproofing chemicals into concrete to reduce permeability. In *Cement and Concrete Research* (Vol. 30, Issue 12, pp. 1969–1977). Elsevier BV. [https://doi.org/10.1016/s0008-8846\(00\)00415-4](https://doi.org/10.1016/s0008-8846(00)00415-4)

[11] Van Tittelboom, K., De Belie, N., Van Loo, D., & Jacobs, P. (2011). Self-healing efficiency of cementitious materials containing tubular capsules filled with healing agent. In *Cement and Concrete Composites* (Vol. 33, Issue 4, pp. 497–505). Elsevier BV. <https://doi.org/10.1016/j.cemconcomp.2011.01.004>

[12] Joseph, C., Jefferson, A. D., Isaacs, B., Lark, R., & Gardner, D. (2010). Experimental investigation of adhesive-based self-healing of cementitious materials. In *Magazine of Concrete Research* (Vol. 62, Issue 11, pp. 831–843). Thomas Telford Ltd. <https://doi.org/10.1680/mac.2010.62.11.831>

[13] Homma, D., Mihashi, H., & Nishiwaki, T. (2009). Self-Healing Capability of Fibre Reinforced Cementitious Composites. In *Journal of Advanced Concrete Technology* (Vol. 7, Issue 2, pp. 217–228). Japan Concrete Institute. <https://doi.org/10.3151/jact.7.217>

- [14] Nishiwaki, T., Koda, M., Yamada, M., Mihashi, H., & Kikuta, T. (2012). c on Self-Healing Capability of FRCC Using Different Types of Synthetic Fibers. In *Journal of Advanced Concrete Technology* (Vol. 10, Issue 6, pp. 195–206). Japan Concrete Institute. <https://doi.org/10.3151/jact.10.195>
- [15] Mauser, T., Déjugnat, C., & Sukhorukov, G. B. (2004). Reversible pH-Dependent Properties of Multilayer Microcapsules Made of Weak Polyelectrolytes. In *Macromolecular Rapid Communications* (Vol. 25, Issue 20, pp. 1781–1785). Wiley. <https://doi.org/10.1002/marc.200400331>
- [16] Liang, K., Such, G. K., Johnston, A. P. R., Zhu, Z., Ejima, H., Richardson, J. J., Cui, J., & Caruso, F. (2013). Endocytic pH-Triggered Degradation of Nanoengineered Multilayer Capsules. In *Advanced Materials* (Vol. 26, Issue 12, pp. 1901–1905). Wiley. <https://doi.org/10.1002/adma.201305144>
- [17] Hammad, N., Elnemr, A., & Shaaban, I. G. (2023). State-of-the-Art Report: The Self-Healing Capability of Alkali-Activated Slag (AAS) Concrete. In *Materials* (Vol. 16, Issue 12, p. 4394). MDPI AG. <https://doi.org/10.3390/ma16124394>
- [18] Dong, B., Wang, Y., Fang, G., Han, N., Xing, F., & Lu, Y. (2015). Smart releasing behaviour of a chemical self-healing microcapsule in the stimulated concrete pore solution. In *Cement and Concrete Composites* (Vol. 56, pp. 46–50). Elsevier BV. <https://doi.org/10.1016/j.cemconcomp.2014.10.006>
- [19] Lv, L., Yang, Z., Chen, G., Zhu, G., Han, N., Schlangen, E., & Xing, F. (2016). Synthesis and characterization of a new polymeric microcapsule and feasibility investigation in self-healing cementitious materials. In *Construction and Building Materials* (Vol. 105, pp. 487–495). Elsevier BV. <https://doi.org/10.1016/j.conbuildmat.2015.12.185>
- [20] Xu, N., Song, Z., Guo, M.-Z., Jiang, L., Chu, H., Pei, C., Yu, P., Liu, Q., & Li, Z. (2021). Employing ultrasonic wave as a novel trigger of microcapsule self-healing cementitious materials. In *Cement and Concrete Composites* (Vol. 118, p. 103951). Elsevier BV. <https://doi.org/10.1016/j.cemconcomp.2021.103951>
- [21] Feng, J., Su, Y., & Qian, C. (2019). Coupled effect of PP fiber, PVA fiber and bacteria on self-healing efficiency of early-age cracks in concrete. In *Construction and Building Materials* (Vol. 228, p. 116810). Elsevier BV. <https://doi.org/10.1016/j.conbuildmat.2019.116810>
- [22] Qiu, J., Tan, H. S., & Yang, E.-H. (2016). Coupled effects of crack width, slag content, and conditioning alkalinity on autogenous healing of engineered cementitious composites. In *Cement and Concrete Composites* (Vol. 73, pp. 203–212). Elsevier BV. <https://doi.org/10.1016/j.cemconcomp.2016.07.013>
- [23] BS-EN197-1, (2011) “Cement Part 1: Composition, Specifications and Conformity Criteria for Common Cements,” Br. Stand., no. November, 2011.
- [24] Egyptian Standards ES 4756-1/2007, Cement Part 1: Composition, Specifications and Conformity Criteria for common cements. Egyptian Organization for Standards & Quality, Arab Republic of Egypt, 2007.
- [25] ASTM C168, (2022). Terminology Relating to Thermal Insulation. ASTM International. <https://doi.org/10.1520/c0168-22>

- 1020 [26] ASTM C33, (2018). Specification for Concrete Aggregates. ASTM International.  
1021 [https://doi.org/10.1520/c0033\\_c0033m-18](https://doi.org/10.1520/c0033_c0033m-18).
- 1022 [27] BS EN 933-1, (2012) "Tests for geometrical properties of aggregates Determination of  
1023 particle size distribution. Sieving method", Br. Stand., 2012
- 1024 [28] ASTM C117, (2017). Test Method for Materials Finer than 75-µm (No. 200) Sieve in  
1025 Mineral Aggregates by Washing. ASTM International. <https://doi.org/10.1520/c0117-17>.
- 1026 [29] ASTM C127, (2015). Test Method for Relative Density (Specific Gravity) and  
1027 Absorption of Coarse Aggregate. ASTM International. <https://doi.org/10.1520/c0127-15>
- 1028 [30] ASTM C128, (2022). Test Method for Relative Density (Specific Gravity) and  
1029 Absorption of Fine Aggregate. ASTM International. <https://doi.org/10.1520/c0128-22>.
- 1030 [31] BS 812-2, (1999) British Standards Institution BSI, "BS 812: Part 2:1995 Testing  
1031 aggregates, Methods of determination of density," Br. Stand., no. 105, 1999.
- 1032 [32] BS 812-103, (1989) "Testing aggregates — Part 103: Method for determination of  
1033 particle size distribution — Section 103.2 Sedimentation test," Br. Stand., no. 1, 1989.
- 1034 [33] Tian, H., Zhang, Y. X., Ye, L., & Yang, C. (2015). Mechanical behaviours of green hybrid  
1035 fibre-reinforced cementitious composites. In Construction and Building Materials (Vol.  
1036 95, pp. 152–163). Elsevier BV. <https://doi.org/10.1016/j.conbuildmat.2015.07.143>.
- 1037 [34] Chen, Y., & Qiao, P. (2011). Crack Growth Resistance of Hybrid Fiber-Reinforced  
1038 Cement Matrix Composites. In Journal of Aerospace Engineering (Vol. 24, Issue 2, pp.  
1039 154–161). American Society of Civil Engineers (ASCE).  
1040 [https://doi.org/10.1061/\(asce\)as.1943-5525.0000031](https://doi.org/10.1061/(asce)as.1943-5525.0000031)
- 1041 [35] Khan, M., Cao, M., & Ali, M. (2020). Cracking behaviour and constitutive modelling of  
1042 hybrid fibre reinforced concrete. In Journal of Building Engineering (Vol. 30, p. 101272).  
1043 Elsevier BV. <https://doi.org/10.1016/j.jobbe.2020.101272>
- 1044 [36] ACI 211.1-91, "Standard Practice for Selecting Proportions for Normal Heavyweight,  
1045 and Mass Concrete (ACI 211.1-91) Reapproved 1997," ACI Comm. Rep., 1997.
- 1046 [37] Srinivasa, C. H., & Venkatesh. (2022). Prediction of Compressive Strength of Polyvinyl  
1047 Alcohol Fiber Reinforced Bendable Concrete. In IOP Conference Series: Earth and  
1048 Environmental Science (Vol. 982, Issue 1, p. 012007). IOP Publishing.  
1049 <https://doi.org/10.1088/1755-1315/982/1/012007>
- 1050 [38] Zhou, S., Zhu, H., Ju, J. W., Yan, Z., & Chen, Q. (2017). Modeling microcapsule-enabled  
1051 self-healing cementitious composite materials using discrete element method. In  
1052 International Journal of Damage Mechanics (Vol. 26, Issue 2, pp. 340–357). SAGE  
1053 Publications. <https://doi.org/10.1177/1056789516688835>
- 1054 [39] British Standards Institution BSI, "Testing hardened concrete - Part 2: Making and curing  
1055 specimens for strength tests," BS En 12390-2 2009, 2009.
- 1056 [40] ASTM C143/C143M, (2012). Test Method for Slump of Hydraulic-Cement Concrete.  
1057 ASTM International. [https://doi.org/10.1520/c0143\\_c0143m-12](https://doi.org/10.1520/c0143_c0143m-12)
- 1058 [41] ASTM C642, (2021). Test Method for Density, Absorption, and Voids in Hardened  
1059 Concrete. ASTM International. <https://doi.org/10.1520/c0642-21>

- [42] Kim, D. J., Park, S. H., Ryu, G. S., & Koh, K. T. (2011). Comparative flexural behaviour of Hybrid Ultra High Performance Fiber Reinforced Concrete with different macro fibers. In *Construction and Building Materials* (Vol. 25, Issue 11, pp. 4144–4155). Elsevier BV. <https://doi.org/10.1016/j.conbuildmat.2011.04.051>
- [43] Sharaky, I. A., Ahmad, S. S., El-Azab, A. M., & Khalil, H. S. (2021). Strength and Mass Loss Evaluation of HSC with Silica Fume and Nano-Silica Exposed to Elevated Temperatures. In *Arabian Journal for Science and Engineering* (Vol. 47, Issue 4, pp. 4187–4209). Springer Science and Business Media LLC. <https://doi.org/10.1007/s13369-021-06006-7>.
- [44] Pakravan, H. R., Latifi, M., & Jamshidi, M. (2014). Ductility improvement of cementitious composites reinforced with polyvinyl alcohol-polypropylene hybrid fibers. In *Journal of Industrial Textiles* (Vol. 45, Issue 5, pp. 637–651). SAGE Publications. <https://doi.org/10.1177/1528083714534712>.
- [45] BS EN 12390-2019 Part 3, “Testing hardened concrete: Compressive strength of test specimens,” Br. Stand. Inst., 2019.
- [46] ASTM C 78, (2009). Test Method for Flexural Strength of Concrete (Using Simple Beam with Third-Point Loading). ASTM International. <https://doi.org/10.1520/c0078-09>.
- [47] Liu, H.-K., Liao, W.-C., Tseng, L., Lee, W.-H., & Sawada, Y. (2004). Compression strength of pre-damaged concrete cylinders reinforced by non-adhesive filament wound composites. In *Composites Part A: Applied Science and Manufacturing* (Vol. 35, Issue 2, pp. 281–292). Elsevier BV. [https://doi.org/10.1016/s1359-835x\(03\)00250-1](https://doi.org/10.1016/s1359-835x(03)00250-1)
- [48] Ma, G., Li, H., Yan, L., & Huang, L. (2018). Testing and analysis of basalt FRP-confined damaged concrete cylinders under axial compression loading. In *Construction and Building Materials* (Vol. 169, pp. 762–774). Elsevier BV. <https://doi.org/10.1016/j.conbuildmat.2018.02.172>
- [49] Mesbah, H.-A., & Benzaid, R. (2017). Damage-based stress-strain model of RC cylinders wrapped with CFRP composites. *Advances in Concrete Construction*, 5(5), 539–561. <https://doi.org/10.12989/ACC.2017.5.5.539>
- [50] Yang, Y., Lepech, M. D., Yang, E.-H., & Li, V. C. (2009). Autogenous healing of engineered cementitious composites under wet–dry cycles. In *Cement and Concrete Research* (Vol. 39, Issue 5, pp. 382–390). Elsevier BV. <https://doi.org/10.1016/j.cemconres.2009.01.013>
- [51] Topič, J., Prošek, Z., Indrová, K., Plachý, T., Nežerka, V., Kopecký, L., & Tesárek, P. (2015). EFFECT OF PVA MODIFICATION ON PROPERTIES OF CEMENT COMPOSITES. In *Acta Polytechnica* (Vol. 55, Issue 1, pp. 64–75). Czech Technical University in Prague - Central Library. <https://doi.org/10.14311/ap.2015.55.0064>
- [52] Hussein, Z. M., Abedali, A. H., & Ahmead, A. S. (2019). Improvement Properties of Self-Healing Concrete by Using Bacteria. In *IOP Conference Series: Materials Science and Engineering* (Vol. 584, Issue 1, p. 012034). IOP Publishing. <https://doi.org/10.1088/1757-899x/584/1/012034>
- [53] Zhang, P., Li, Q., Wang, J., Shi, Y., & Ling, Y. (2019). Effect of PVA fiber on durability of cementitious composite containing nano-SiO<sub>2</sub>. In *Nanotechnology Reviews* (Vol. 8,



1102 Issue 1, pp. 116–127). Walter de Gruyter GmbH. [https://doi.org/10.1515/ntrev-2019-](https://doi.org/10.1515/ntrev-2019-0011)  
1103 0011

1104 [54] Safiuddin, M., Ihteshaam, S., Kareem, R. A., & Shalam. (2022). A study on self-healing  
1105 concrete. In *Materials Today: Proceedings* (Vol. 52, pp. 1175–1181). Elsevier BV.  
1106 <https://doi.org/10.1016/j.matpr.2021.11.023>

1107 [55] Flatt R, Houst Y, Bowen P and HofmannH2000 Electrostatic repulsion induced by  
1108 superplasticizers between cement particles – an overlooked mechanism?  
1109 Sixth CANMET/ACI Int. Conf. on Superplasticizers and Other Chemical Admixtures in  
1110 Concrete 195, 29–42

1111 [56] Neville, A.M. and Brooks, J.J. (2010) *Concrete Technology*. 2nd Edition, Pearson  
1112 Education Ltd., London.

1113 [57] Yew, M. K., Bin Mahmud, H., Ang, B. C., & Yew, M. C. (2015). Effects of Low Volume  
1114 Fraction of Polyvinyl Alcohol Fibers on the Mechanical Properties of Oil Palm Shell  
1115 Lightweight Concrete. In *Advances in Materials Science and Engineering* (Vol. 2015, pp.  
1116 1–11). Hindawi Limited. <https://doi.org/10.1155/2015/425236>

1117 [58] Shafigh, P., Mahmud, H., & Jumaat, M. Z. (2011). Effect of steel fiber on the mechanical  
1118 properties of oil palm shell lightweight concrete. In *Materials & Design* (Vol. 32,  
1119 Issue 7, pp. 3926–3932). Elsevier BV. <https://doi.org/10.1016/j.matdes.2011.02.055>

1120 [59] Zhang, C., Liu, R., Chen, M., Li, X., & Zhu, Z. (2022). Coupled effect of self-healing  
1121 granules and permeable crystalline additive on early-age cracks repair in cement material.  
1122 In *Materials Letters* (Vol. 323, p. 132560). Elsevier BV.  
1123 <https://doi.org/10.1016/j.matlet.2022.132560>

1124 [60] Bhaskar, S., Anwar Hossain, K. M., Lachemi, M., Wolfaardt, G., & Otini Kroukamp, M.  
1125 (2017). Effect of self-healing on strength and durability of zeolite-immobilized bacterial  
1126 cementitious mortar composites. In *Cement and Concrete Composites* (Vol. 82, pp. 23–  
1127 33). Elsevier BV. <https://doi.org/10.1016/j.cemconcomp.2017.05.013>.

1128 [61] Luo, M., Qian, C., & Li, R. (2015). Factors affecting crack repairing capacity of bacteria-  
1129 based self-healing concrete. In *Construction and Building Materials* (Vol. 87, pp. 1–7).  
1130 Elsevier BV. <https://doi.org/10.1016/j.conbuildmat.2015.03.117>.

1131 [62] Fabbri, A., Corvisier, J., Schubnel, A., Brunet, F., Goffé, B., Rimmelé, G., & Barlet-  
1132 Gouédard, V. (2009). Effect of carbonation on the hydro-mechanical properties of  
1133 Portland cements. In *Cement and Concrete Research* (Vol. 39, Issue 12, pp. 1156–1163).  
1134 Elsevier BV. <https://doi.org/10.1016/j.cemconres.2009.07.028>

1135 [63] Pei, R., Liu, J., Wang, S., & Yang, M. (2013). Use of bacterial cell walls to improve the  
1136 mechanical performance of concrete. In *Cement and Concrete Composites* (Vol. 39, pp.  
1137 122–130). Elsevier BV. <https://doi.org/10.1016/j.cemconcomp.2013.03.024>

1138 [64] Johannesson, B., & Utgenannt, P. (2001). Microstructural changes caused by carbonation  
1139 of cement mortar. In *Cement and Concrete Research* (Vol. 31, Issue 6, pp. 925–931).  
1140 Elsevier BV. [https://doi.org/10.1016/s0008-8846\(01\)00498-7](https://doi.org/10.1016/s0008-8846(01)00498-7)

1141 [65] Kakooei, S., Akil, H. M., Jamshidi, M., & Rouhi, J. (2012). The effects of polypropylene  
1142 fibers on the properties of reinforced concrete structures. In *Construction and Building*



Materials (Vol. 27, Issue 1, pp. 73–77). Elsevier BV.  
<https://doi.org/10.1016/j.conbuildmat.2011.08.015>

[66] Sambudi, N. S., Park, S. B., & Cho, K. (2016). Enhancing the mechanical properties of electrospun chitosan/poly(vinyl alcohol) fibers by mineralization with calcium carbonate. In *Journal of Materials Science* (Vol. 51, Issue 16, pp. 7742–7753). Springer Science and Business Media LLC. <https://doi.org/10.1007/s10853-016-0056-8>.

[67] Chen, H., Qian, C., & Huang, H. (2016). Self-healing cementitious materials based on bacteria and nutrients immobilized respectively. In *Construction and Building Materials* (Vol. 126, pp. 297–303). Elsevier BV. <https://doi.org/10.1016/j.conbuildmat.2016.09.023>.

[68] Wang, J., Van Tittelboom, K., De Belie, N., & Verstraete, W. (2012). Use of silica gel or polyurethane immobilized bacteria for self-healing concrete. In *Construction and Building Materials* (Vol. 26, Issue 1, pp. 532–540). Elsevier BV. <https://doi.org/10.1016/j.conbuildmat.2011.06.054>

[69] Shaaban, S., Hammad, N., Elnemr, A., & Shaaban, I. G. (2023). Efficiency of Bacteria-Based Self-Healing Mechanism in Concrete. In *Materials Science Forum* (Vol. 1089, pp. 135–143). Trans Tech Publications, Ltd. <https://doi.org/10.4028/p-tc6w54>.

[70] Jain, N., Singh, V. K., & Chauhan, S. (2017). A review on mechanical and water absorption properties of polyvinyl alcohol-based composites/films. In *Journal of the Mechanical Behaviour of Materials* (Vol. 26, Issues 5–6, pp. 213–222). Walter de Gruyter GmbH. <https://doi.org/10.1515/jmbm-2017-0027>

[71] Shen, Y., Li, Q., Xu, S., & Liu, X. (2021). Electromagnetic wave absorption of multifunctional cementitious composites incorporating polyvinyl alcohol (PVA) fibers and fly ash: Effects of microstructure and hydration. In *Cement and Concrete Research* (Vol. 143, p. 106389). Elsevier BV. <https://doi.org/10.1016/j.cemconres.2021.106389>

[72] Li, Z., Wang, X., Yan, W., Ding, L., Liu, J., Wu, Z., & Huang, H. (2023). Physical and mechanical properties of gypsum-based composites reinforced with basalt, glass, and PVA fibers. In *Journal of Building Engineering* (Vol. 64, p. 105640). Elsevier BV. <https://doi.org/10.1016/j.jobbe.2022.105640>

[73] Alderete, N. M., Villagrán Zaccardi, Y. A., & De Belie, N. (2019). Physical evidence of swelling as the cause of anomalous capillary water uptake by cementitious materials. In *Cement and Concrete Research* (Vol. 120, pp. 256–266). Elsevier BV. <https://doi.org/10.1016/j.cemconres.2019.04.001>

[74] Martys, N. S., & Ferraris, C. F. (1997). Capillary transport in mortars and concrete. *Cement and concrete research*, 27(5), 747–760.

[75] Aly, T., Sanjayan, J. G., & Collins, F. (2008). Effect of polypropylene fibers on shrinkage and cracking of concretes. In *Materials and Structures* (Vol. 41, Issue 10, pp. 1741–1753). Springer Science and Business Media LLC. <https://doi.org/10.1617/s11527-008-9361-2>

[76] Akhavan, A., Shafaatian, S.-M.-H., & Rajabipour, F. (2012). Quantifying the effects of crack width, tortuosity, and roughness on water permeability of cracked mortars. In *Cement and Concrete Research* (Vol. 42, Issue 2, pp. 313–320). Elsevier BV. <https://doi.org/10.1016/j.cemconres.2011.10.002>

- 1185 [77] Bear, J. (2013). Dynamics of fluids in porous media. Courier Corporation.
- 1186 [78] Bamigboye, G. O., Ademola, D., Kareem, M., Orogade, B., Odetoyan, A., & Adeniyi,  
 1187 A. (2022). Durability assessment of recycled aggregate in concrete production. In The  
 1188 Structural Integrity of Recycled Aggregate Concrete Produced with Fillers and Pozzolans  
 1189 (pp. 445–467). Elsevier. <https://doi.org/10.1016/b978-0-12-824105-9.00010-x>
- 1190 [79] R. Siddique and R. Belarbi, (2022). Sustainable Concrete Made with Ashes and Dust from  
 1191 Different Sources. (2022). Elsevier. <https://doi.org/10.1016/c2020-0-01219-3>.
- 1192 [80] ASTM C1585, (2013). Test Method for Measurement of Rate of Absorption of Water by  
 1193 Hydraulic- Cement Concretes. ASTM International. <https://doi.org/10.1520/c1585-13>
- 1194 [81] Ataie, F. F., Juenger, M. C. G., Taylor-Lange, S. C., & Riding, K. A. (2015). Comparison  
 1195 of the retarding mechanisms of zinc oxide and sucrose on cement hydration and  
 1196 interactions with supplementary cementitious materials. In Cement and Concrete  
 1197 Research (Vol. 72, pp. 128–136). Elsevier BV.  
 1198 <https://doi.org/10.1016/j.cemconres.2015.02.023>
- 1199 [82] Xu, Y., Zhang, X., Ma, B., & Liao, X. (2011). Effects of Temperature on the Performance  
 1200 of Sucrose in Cement Hydration. In Journal of Materials in Civil Engineering (Vol. 23,  
 1201 Issue 7, pp. 1124–1127). American Society of Civil Engineers (ASCE).  
 1202 [https://doi.org/10.1061/\(asce\)mt.1943-5533.0000264](https://doi.org/10.1061/(asce)mt.1943-5533.0000264).